

Dicke-state preparation through global transverse control of Ising-coupled qubitsVladimir M. Stojanović  and Julian K. Nauth *Institut für Angewandte Physik, Technical University of Darmstadt, D-64289 Darmstadt, Germany*

(Received 20 February 2023; accepted 2 June 2023; published 7 July 2023)

We consider the problem of engineering the two-excitation Dicke state $|D_2^3\rangle$ in a three-qubit system with all-to-all Ising-type qubit-qubit interaction, which is also subject to global transverse (Zeeman-type) control fields. The theoretical underpinning for our envisioned state-preparation scheme, in which $|000\rangle$ is adopted as the initial state of the system, is provided by a Lie-algebraic result that guarantees state-to-state controllability of this system for an arbitrary choice of initial and final states that are invariant with respect to permutations of qubits. This scheme is envisaged in the form of a pulse sequence that involves three instantaneous control pulses, which are equivalent to global qubit rotations, and two Ising-interaction pulses of finite durations between consecutive control pulses. The design of this pulse sequence (whose total duration is $T \approx 0.95 \hbar/J$, where J is the Ising-coupling strength) leans heavily on the concept of the symmetric sector, a four-dimensional, permutationally invariant subspace of the three-qubit Hilbert space. We demonstrate the feasibility of the proposed state-preparation scheme by carrying out a detailed numerical analysis of its robustness to systematic errors, i.e., deviations from the optimal values of the eight parameters that characterize the underlying pulse sequence. Finally, we discuss how our proposed scheme can be generalized for engineering Dicke states in systems with $N \geq 4$ qubits. For the sake of illustration, we describe the preparation of the two-excitation Dicke state $|D_2^4\rangle$ in a four-qubit system.

DOI: [10.1103/PhysRevA.108.012608](https://doi.org/10.1103/PhysRevA.108.012608)**I. INTRODUCTION**

Advanced capabilities in quantum-state engineering [1–28] represent one of the crucial prerequisites for the development of next-generation quantum technologies [29]. Tantalizing achievements have been reported in this thriving research area in recent years, pertaining—in particular—to the creation of highly entangled quantum states in systems of increasingly large size that belong to various physical platforms for quantum computing (QC) [12,30,31]. Two of the most widely discussed classes of such states are maximally-entangled multipartite states of W [32] and Greenberger-Horne-Zeilinger (GHZ) [33] types. Motivated primarily by their proven utility in various quantum-information processing [34] tasks, a multitude of proposals have been made in recent years for the efficient generation of both W [1–11] and GHZ [12–20] states in diverse QC platforms. In addition, deterministic interconversions of W and GHZ states have lately also been attracting considerable attention [23–28].

Dicke states, originally introduced in connection with the phenomenon of superradiance [35], represent yet another important family of highly entangled multiqubit states. Owing to their favorable properties—such as robustness to particle loss [36] and immunity to collective dephasing noise [37]—they hold promise for emerging quantum-technology applications in areas as diverse as quantum networking [38], quantum metrology [39], quantum game theory [40], and quantum combinatorial optimization [41]. The a -excitation Dicke state $|D_a^N\rangle$ of an N -qubit system is an equal-weight superposition of all N -qubit states with Hamming weight of a (i.e. all binary bitstrings of length N with exactly a appearances of 1); this family of states includes W states as its special, single-excitation ($a = 1$) case, i.e. $|D_1^N\rangle \equiv |W_N\rangle$. Several schemes

have heretofore been proposed for the experimental realization of Dicke states in various physical platforms, such as trapped ions [42–44], neutral atoms [45–47], photons [38,48], superconducting qubits [49], and spin ensembles [50].

In this paper, we consider the problem of engineering the two-excitation Dicke state $|D_2^3\rangle$ in a three-qubit system with long-ranged (all-to-all) Ising-type (zz) interaction between qubits, which are acted upon by global, Zeeman-type control fields in the transverse (x and y) directions. Aside from quantum-technology applications of Dicke states, the motivation behind the present work stems from the fact that qubit arrays with Ising-type qubit-qubit interaction can be realized in several physical platforms for QC [51]. One familiar example is furnished by nuclear spins, i.e., nuclear-magnetic-resonance (NMR) systems [52–54]. Another example are capacitively coupled spin qubits of singlet-triplet type [55], formed using double quantum dots [56]. Finally, arrays of optically trapped neutral atoms interacting via off-resonant dipole-dipole (van der Waals) interactions feature an all-to-all Ising-type interaction between neutral-atom qubits based on Rydberg states [57,58]. This last, neutral-atom-based platform offers particularly rich possibilities for quantum-state engineering [59].

A recent result in the realm of Lie-algebraic controllability implies that a qubit array with all-to-all Ising-type interaction between qubits, when acted upon by two global transverse control fields, is state-to-state controllable if the initial and final states are invariant under an arbitrary permutation of qubits [60]; moreover, it is important to note that both our adopted initial state $|000\rangle$ and the sought-after Dicke state $|D_2^3\rangle$ are indeed permutationally invariant. Thus, this last Lie-algebraic result guarantees the existence of a quantum-

control protocol for the preparation of the state $|D_3^2\rangle$ starting from $|000\rangle$ for Ising-coupled qubits with global transverse control.

Our envisaged state-preparation scheme is based on an NMR-type pulse sequence. This pulse sequence turns out to involve three instantaneous (δ -shaped) global control pulses, two of which correspond to global qubit rotations around the y axis and the remaining one around the x axis, and two Ising-interaction pulses of equal durations between consecutive control pulses. It is worthwhile to mention that NMR-type pulse sequences have heretofore been used in various QC problems [61–68], even in the presence of the same (Ising) type of qubit-qubit interaction. For instance, they were utilized for preserving cluster states [66] in measurement-based QC [69]; the practical usefulness of the Ising-type qubit-qubit coupling in this regard stems from the close kinship between its native two-qubit gate and controlled- Z [34], the gate used for generating cluster states [69].

The design of the envisaged pulse sequence relies heavily on the permutational invariance of the state-preparation problem at hand, more precisely, on the use of the four-dimensional, permutationally invariant subspace (symmetric sector) of the three-qubit Hilbert space. After finding the optimal values of the eight parameters characterizing this pulse sequence (namely, the durations of the interaction pulses, the global-rotation angles, which are related to the control-field magnitudes, and, finally, the angles specifying the directions of the rotation axes in the x - y plane), we carry out a detailed numerical analysis of its sensitivity against systematic errors in the values of those parameters. We show that even for fairly large relative errors in different parameter values, one can still retain Dicke-state fidelities very close to unity, which speaks in favor of the robustness of the proposed scheme.

The remaining part of this paper is organized in the following manner. In Sec. II, the Ising-coupled qubit system at hand and the Dicke-state preparation problem to be addressed in what follows are described in detail; the notation to be used throughout the paper is also introduced, along with some permutational-symmetry-related considerations. Section III is set aside for the discussion of the design of the sought-after NMR-type pulse sequence that allows an efficient Dicke-state preparation. The obtained results for the idealized pulse sequence, i.e., for the optimal values of its eight characteristic parameters, are then presented and discussed. Finally, a geometric interpretation of the proposed pulse sequence, based on a dimensional reduction of the problem at hand and the concept of the Bloch sphere, is also provided. In Sec. IV the robustness of the proposed scheme to systematic errors in its characteristic parameters is discussed in great detail. Section V is concerned with the generalization of the proposed state-preparation scheme to systems with four or more qubits; it starts with some general symmetry-related considerations, followed by the demonstration of the pulse sequence for realizing the two-excitation Dicke state in a four-qubit system. Before closing, in Sec. VI we summarize the main findings of this paper and indicate possible directions for future work. The derivation of the time-evolution operators corresponding to the different stages of the proposed pulse sequences in the three- and four-qubit cases is relegated to the Appendix.

II. SYSTEM AND DICKE-STATE PREPARATION PROBLEM

To set the stage for further discussion, we start by introducing a system of Ising-coupled qubits with global transverse control, with emphasis on the relevant Lie-algebraic controllability results (Sec. II A). We then briefly review some basic properties of Dicke states and formulate the state-preparation problem under consideration as a quantum-control problem in a three-qubit system (Sec. II B). Finally, we underscore the consequences of the permutational invariance of the system at hand for the solution of this quantum-control problem (Sec. II C).

A. Hamiltonian of Ising-coupled qubit arrays with global transverse control

The system at hand is an array of qubits coupled through long-range (all-to-all) Ising (zz) coupling, which are also acted upon by global Zeeman-type control fields in the two transverse (x and y) directions. Accordingly, the total system Hamiltonian $H(t) = H_{ZZ} + H_C(t)$ is given by the sum of the Ising-interaction part H_{ZZ} and the control part, i.e.,

$$H(t) = H_{ZZ} + h_x(t)\mathcal{X} + h_y(t)\mathcal{Y}, \quad (1)$$

where $h_x(t)$ and $h_y(t)$ are global control fields in the x and y directions, respectively. The operators H_{ZZ} , \mathcal{X} , and \mathcal{Y} are given by

$$H_{ZZ} = J \sum_{1 \leq n < n' \leq N} Z_n Z_{n'}, \quad (2)$$

$$\mathcal{X} = \sum_{n=1}^N X_n, \quad \mathcal{Y} = \sum_{n=1}^N Y_n, \quad (3)$$

where J denotes the Ising coupling strength, while X_n , Y_n , and Z_n are the Pauli operators of the n th qubit ($n = 1, \dots, N$), i.e.,

$$\mathbf{X}_n = \mathbb{1}_2 \otimes \dots \otimes \mathbb{1}_2 \otimes \underbrace{\mathbf{X}}_n \otimes \mathbb{1}_2 \otimes \dots \otimes \mathbb{1}_2, \quad (4)$$

where $\mathbf{X} \equiv (X, Y, Z)^T$ is the vector of single-qubit Pauli operators and $\mathbf{X}_n \equiv (X_n, Y_n, Z_n)^T$ its counterpart acting on the N -qubit Hilbert space; $\mathbb{1}_2$ is the single-qubit identity operator.

The Lie-algebraic controllability of coupled spin-1/2 chains (qubit arrays) was discussed extensively in the past [70]. In particular, for complete (operator) controllability, i.e., the capability of realizing an arbitrary unitary transformation on the Hilbert space of the underlying system, which is tantamount to enabling universal QC, of a qubit array with Ising-type interaction it is necessary to have two mutually noncommuting control fields acting on every qubit in the array [71]. Therefore, an N -qubit system with Ising-type coupling between qubits and acted upon by global Zeeman-type control fields in the x and y directions [cf. Eqs. (1) to (3) above] is, generally speaking, not completely operator-controllable; rephrasing, its corresponding dynamical Lie algebra [70] $\mathcal{L}_d = \text{span}\{H_{ZZ}, \mathcal{X}, \mathcal{Y}\}$ is not isomorphic with the full $u(2^N)$ or $su(2^N)$ algebra, being, in fact, isomorphic with one of their proper Lie subalgebras.

An important controllability-related result for Ising-coupled qubit arrays was recently derived, which is based on the invariance under permutations of qubits. Namely, it has been shown that a system described by the permutationally invariant Hamiltonian of Eq. (1) is completely state-to-state controllable for an arbitrary pair of permutationally invariant initial and final states [60]. In other words, the time dependence of global control fields $h_x(t)$ and $h_y(t)$ [cf. Eq. (1)] can, in principle, be found such that an arbitrary permutationally invariant final state can be reached in a finite time starting from a permutationally invariant initial state. However (as is also the case with other results in the realm of Lie-algebraic controllability [70], which have the nature of existence theorems), the aforementioned recent result does not provide the actual time dependence of the fields $h_x(t)$ and $h_y(t)$ that allows this system to evolve from a chosen initial to a desired final state [72].

B. Preparation of the Dicke state $|D_2^3\rangle$ as a quantum-control problem

In the following, we formulate the envisaged deterministic preparation of the two-excitation Dicke state $|D_2^3\rangle$ in a three-qubit system ($N = 3$), starting from the state $|000\rangle$, as a quantum-control problem. To begin with, we provide a short reminder on the basic properties of Dicke states.

A generic N -qubit state with a excitations (i.e., a qubits in the logical state $|1\rangle$, with the remaining ones being in the state $|0\rangle$) can be parameterized as $\{|n_1, \dots, n_a\rangle\}$, with n_1, \dots, n_a enumerating those qubits that are in the logical state $|1\rangle$. The a -excitation Dicke state of an N -qubit system is given by

$$|D_a^N\rangle = \binom{N}{a}^{-1/2} \sum_{n_1 < \dots < n_a} | \{n_1, \dots, n_a\} \rangle, \quad (5)$$

i.e., by the equal-weight superposition of all the states $\{|n_1, \dots, n_a\rangle\}$ spanning the subspace of the N -qubit states with exactly a excitations (i.e., states corresponding to bit strings of Hamming weight a); the sum in Eq. (5) runs over all $\binom{N}{a}$ combinations of a qubits out of N .

While the notation used in Eq. (5) is appropriate for the most general Dicke states, for relatively small values of N one can resort to a simpler notation. In particular, the two-excitation Dicke state of $N = 3$ qubits, the state of primary interest in the present work, can be written as

$$|D_2^3\rangle = \frac{1}{\sqrt{3}} (|110\rangle + |101\rangle + |011\rangle). \quad (6)$$

Our treatment in what follows will rely heavily on the permutational invariance of this state (see Sec. II C below).

In the special case $N = 3$ the Ising-interaction Hamiltonian [cf. Eq. (2)] reduces to

$$H_{ZZ} = J(Z_1Z_2 + Z_2Z_3 + Z_1Z_3), \quad (7)$$

while the total control Hamiltonian is given by

$$H_C(t) = h_x(t)(X_1 + X_2 + X_3) + h_y(t)(Y_1 + Y_2 + Y_3). \quad (8)$$

Our objective in the following is to find the time dependence of control fields $h_x(t)$ and $h_y(t)$ such that the dynamics governed by the total Hamiltonian $H(t) = H_{ZZ} + H_C(t)$ allows the preparation of the state $|D_2^3\rangle$ in a finite time starting from the state $|000\rangle$. Thus, the state $|\psi(t)\rangle$ of the three-qubit system under consideration ought to satisfy the conditions

$$|\psi(t = 0)\rangle = |000\rangle, \quad |\psi(t = T)\rangle = |D_2^3\rangle, \quad (9)$$

where T is the as-yet-unknown state-preparation time.

C. Symmetric sector of the three-qubit Hilbert space and its basis

Before embarking on the design of the pulse sequence for implementing the desired Dicke-state preparation, it is pertinent to explore the consequences of the permutational invariance of the problem under consideration. Particularly useful in this regard is the concept of the symmetric sector of the three-qubit Hilbert space.

In the quantum-control context, it is often beneficial to consider pure states that are invariant with respect to permutations of qubits [73–75], either under the full symmetric group S_N (where N is the number of qubits) or with respect to proper subgroups of S_N [76]. In particular, in the state-preparation problem under consideration we focus on the subset of all the unitaries on the Hilbert space $\mathcal{H} \equiv (\mathbb{C}^2)^{\otimes 3}$ of the system at hand that are invariant under the full permutation group S_3 . The relevant (permutationally invariant) Lie subgroup $U^{S_3}(8)$ of $U(8)$ has dimension 20 [60]. Its associated Lie algebra is $u^{S_3}(8) = \text{span}\{i\Pi(\sigma_1 \otimes \sigma_2 \otimes \sigma_3)\}$, where $\Pi = (3!)^{-1} \sum_{P \in S_3} P$ and σ_n ($n = 1, 2, 3$) stands either for $\mathbb{1}_2$ or one of the Pauli operators.

The eight-dimensional total Hilbert space \mathcal{H} of a three-qubit system decomposes into three invariant subspaces under the action of $u^{S_3}(8)$. Among those subspaces, which correspond to irreducible representations of $su(2)$, there are two subspaces of dimension 2 and one that has dimension 4. The four-dimensional subspace comprises the states that are invariant under an arbitrary permutation of qubits, hence being referred to as the symmetric sector [74]. The states

$$\begin{aligned} |\zeta_0\rangle &= |000\rangle, \quad |\zeta_1\rangle = \frac{1}{\sqrt{3}} (|100\rangle + |010\rangle + |001\rangle), \\ |\zeta_2\rangle &= \frac{1}{\sqrt{3}} (|110\rangle + |101\rangle + |011\rangle), \quad |\zeta_3\rangle = |111\rangle, \end{aligned} \quad (10)$$

form an orthonormal, symmetry-adapted basis of the symmetric sector [27,60], where the subscript a in $|\zeta_a\rangle$ is equal to the Hamming weight of the corresponding bit string. These four states are, in fact, the four Dicke states $|D_a^3\rangle$ ($a = 0, \dots, 3$).

The initial and final states of our envisioned state-preparation scheme [cf. Eq. (9)] correspond to two of the basis states in Eq. (10). While the initial state $|000\rangle \equiv$ corresponds to $|\zeta_0\rangle \equiv |D_0^3\rangle$, the Dicke state $|D_2^3\rangle$ coincides with $|\zeta_2\rangle$. Therefore, it is pertinent to investigate the state-preparation problem at hand within the symmetric sector. To this end, we first map the four basis states in Eq. (10) onto column

vectors [27]:

$$\begin{aligned} |\zeta_0\rangle &\mapsto \begin{pmatrix} 1 \\ 0 \\ 0 \\ 0 \end{pmatrix}, & |\zeta_1\rangle &\mapsto \begin{pmatrix} 0 \\ 1 \\ 0 \\ 0 \end{pmatrix}, \\ |\zeta_2\rangle &\mapsto \begin{pmatrix} 0 \\ 0 \\ 1 \\ 0 \end{pmatrix}, & |\zeta_3\rangle &\mapsto \begin{pmatrix} 0 \\ 0 \\ 0 \\ 1 \end{pmatrix}. \end{aligned} \quad (11)$$

III. PULSE SEQUENCE FOR DICKE-STATE PREPARATION

In the following, we first describe the construction of the NMR-type pulse sequence that allows one to efficiently prepare the desired Dicke state $|D_2^3\rangle$ starting from the state $|000\rangle$ and present the optimal values of its characteristic parameters (Sec. III A). We then discuss the feasibility of realizing the proposed state-preparation scheme with neutral-atom qubits (based on Rydberg states [77]), even in the presence of motion-induced dephasing and ionization effects (Sec. III B). Finally, we provide a geometrical interpretation of this pulse sequence based on a dimensional reduction of the problem to a two-dimensional subspace of the original three-qubit Hilbert space and the concept of the Bloch sphere (Sec. III C).

As indicated above, the sought-after Dicke state is invariant with respect to permutations of qubits. Therefore, the state-preparation problem at hand can be reduced to a four-dimensional subspace (symmetric sector) of the three-qubit Hilbert space and formulated using the basis given in Eq. (10). We hereafter also set $\hbar = 1$, thus all the timescales in the problem under consideration will be expressed in terms of the inverse Ising-coupling strength J^{-1} .

A. Layout of the pulse sequence and the optimal parameter values

In what follows, we aim to find a solution of the state-preparation problem under consideration [cf. Eq. (9)] that has the form of an NMR-type pulse sequence; such pulse sequences typically comprise a certain number of instantaneous (δ -shaped) global control pulses and interaction pulses between consecutive control pulses. More specifically yet, we assume that the pulse sequence of interest here consists of three such control pulses in transverse directions (at times $t = 0$, $t = T_m$, and $t = T$) and two Ising-interaction pulses (a pictorial illustration of this pulse sequence is given in Fig. 1). The transverse (global) control field $\mathbf{h}(t) \equiv [h_x(t), h_y(t), 0]^T$ can then be written in the form

$$\mathbf{h}(t) = \boldsymbol{\alpha}_1 \delta(t) + \boldsymbol{\alpha}_2 \delta(t - T_m) + \boldsymbol{\alpha}_3 \delta(t - T), \quad (12)$$

where the presence of the delta functions in the last equation captures the instantaneous character of the envisioned control pulses and $\boldsymbol{\alpha}_1, \boldsymbol{\alpha}_2, \boldsymbol{\alpha}_3$ are, in principle, arbitrary vectors in the x - y plane. The directions of these vectors are specified by their respective polar angles (azimuths) ϕ_1, ϕ_2, ϕ_3 .

To understand the connection between instantaneous global control pulses in the system at hand and global

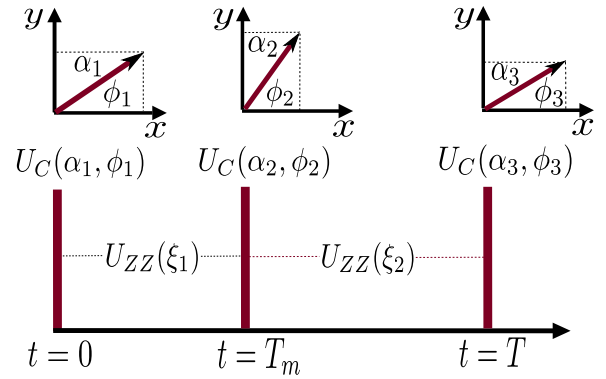


FIG. 1. Schematic of the pulse sequence for the preparation of the Dicke state $|D_2^3\rangle$, which consists of three instantaneous global control pulses and two Ising-interaction pulses. The control pulse characterized by the vector $\boldsymbol{\alpha}_j$ ($j = 1, 2, 3$) in the x - y plane corresponds to a global qubit rotation through an angle of $2\alpha_j$ around the axis whose direction is determined by the unit vector $\hat{\mathbf{n}}_j \equiv (\cos \phi_j, \sin \phi_j, 0)^T$; the polar angles ϕ_j are restricted to values in $[0, \pi)$, while positive (negative) values of α_j correspond to counterclockwise (clockwise) rotations. Here $U_C(\boldsymbol{\alpha}_j) \equiv U_C(\alpha_j, \phi_j)$ are the time-evolution operators corresponding to these control pulses; $U_{ZZ}(\xi_1)$ and $U_{ZZ}(\xi_2)$ are their counterparts pertaining to the interaction pulses, with $\xi_1 \equiv JT_m$ and $\xi_2 \equiv J(T - T_m)$ being their respective dimensionless durations.

rotations it is useful to recall the well-known identity

$$\exp[-i\theta(\hat{\mathbf{n}} \cdot \mathbf{X})] = \cos \theta \mathbb{1}_2 - i \sin \theta (\hat{\mathbf{n}} \cdot \mathbf{X}), \quad (13)$$

for the single-qubit rotation operators $R_{\hat{\mathbf{n}}}(2\theta) \equiv \exp[-i\theta(\hat{\mathbf{n}} \cdot \mathbf{X})]$, where $\hat{\mathbf{n}}$ is an arbitrary unit vector. Based on the last identity it is straightforward to infer that an instantaneous control pulse described by the vector $\boldsymbol{\alpha}_j$ ($j = 1, 2, 3$) corresponds to a global rotation through an angle of $2\alpha_j$ around the axis whose direction is determined by the unit vector $\hat{\mathbf{n}}_j \equiv (\cos \phi_j, \sin \phi_j, 0)^T$. We choose the convention according to which the angles ϕ_j are restricted to values in $[0, \pi)$, while positive (negative) values of α_j correspond to counterclockwise (clockwise) rotations.

It is appropriate to comment at this point on the feasibility of realizing pulse sequences of the proposed form, which involve global instantaneous control pulses, in different physical platforms for QC. First, it should be stressed that the assumption about the instantaneous character of control pulses is well justified in systems where the magnitude of control fields is much larger than the qubit-qubit coupling strength. This last requirement is satisfied for typical control fields of magnetic origin used in the NMR domain [52], as well as for control fields used in superconducting-qubit- [63] and neutral-atom systems [57]. Second, the global character of control pulses (leading to global qubit rotations) constitutes a necessity in several QC platforms of current interest. A typical example are neutral-atom QC setups, where the role of two relevant logical qubit states is played either by two hyperfine states or by a ground state and a high-lying Rydberg state. In such systems one typically makes use of a global microwave field to perform a rotation in the x - y plane on every qubit [78]. This rotation gate has to be global in character because the distance

between qubits in such systems is several orders of magnitude smaller than the wavelength of the microwave field.

The explicit expressions for the time-evolution operators $U_C(\alpha_j) \equiv U_C(\alpha_j, \phi_j)$ ($j = 1, 2, 3$) corresponding to the three global control pulses, as well as their Ising-interaction counterparts $U_{ZZ}(\xi_i)$ with respective dimensionless (defined in units of J^{-1}) durations ξ_i ($i = 1, 2$), in the symmetry-adapted basis of Eq. (10) are straightforward to derive (for a detailed derivation, see the Appendix). By making use of those expressions, we can recover the full time-evolution operator

$$\begin{aligned} \mathcal{U}_{\text{PS}}(\xi_1, \xi_2, \alpha_1, \alpha_2, \alpha_3) &= U_C(\alpha_3)U_{ZZ}(\xi_2)U_C(\alpha_2) \\ &\times U_{ZZ}(\xi_1)U_C(\alpha_1) \end{aligned} \quad (14)$$

describing the envisioned pulse sequence (for a pictorial illustration, see Fig. 1).

Aiming to prepare the state $|D_2^3\rangle$ starting from the initial state $|000\rangle$, we maximize the figure of merit of relevance here (the Dicke-state fidelity \mathcal{F}_D) with respect to the eight pulse-sequence parameters ($\xi_1, \xi_2, \alpha_1, \alpha_2, \alpha_3, \phi_1, \phi_2, \phi_3$). This fidelity is given by the module of the overlap of the target state $|D_2^3\rangle$ and the actual final state $\mathcal{U}_{\text{PS}}(\xi_1, \xi_2, \alpha_1, \alpha_2, \alpha_3)|000\rangle$ of the three-qubit system that results from the application of the pulse sequence [cf. Eq. (14)]

$$\mathcal{F}_D = \left| \langle D_2^3 | \mathcal{U}_{\text{PS}}(\xi_1, \xi_2, \alpha_1, \alpha_2, \alpha_3) | 000 \rangle \right|. \quad (15)$$

We numerically optimize the Dicke-state fidelity in Eq. (15) by making use of the minimize routine from the `scipy.optimize` package of the SCIPY library [79]. In this way, we obtain the following optimal values of the eight pulse-sequence parameters:

$$\begin{aligned} \alpha_{1,0} &= 3\pi/4, \\ \alpha_{2,0} &= -\arccos(1/3)/4, \\ \alpha_{3,0} &= \pi/4, \\ \phi_{1,0} &= \phi_{3,0} = \pi/2, \quad \phi_{2,0} = 0, \\ \xi_{1,0} &= \xi_{2,0} = [\pi - \arccos(1/3)]/4. \end{aligned} \quad (16)$$

Based on the obtained results, we can specify the x and y components of the global control field $\mathbf{h}(t)$ [whose assumed general form is given in Eq. (12)] that are required for the preparation of the state $|D_2^3\rangle$ in the system at hand:

$$\begin{aligned} h_x(t) &= -\frac{J}{4} \arccos(1/3) \delta(t - T_m), \\ h_y(t) &= \frac{\pi J}{4} [3 \delta(t) + \delta(t - T)]. \end{aligned} \quad (17)$$

Thus, the x component of the obtained global control field has the form of an instantaneous pulse at $t = T_m$, while its counterpart in the y direction entails two such pulses, at times $t = 0$ and $t = T$.

From the obtained optimal parameter values [cf. Eq. (16)], the following conclusions can be drawn. First, the first and third control pulses correspond to global rotations around the y axis, with the respective rotation angles of $3\pi/2$ and $\pi/2$. Second, the second control pulse corresponds to a global rotation around the x axis through an angle of $\arccos(1/3)/2$. Finally, the two interaction pulses have equal durations. Given that the pulse sequence involves instantaneous control pulses,

the total duration T of the pulse sequence, i.e., the state-preparation time, is given by $T = 2\xi_{1,0} J^{-1}$, which amounts to $T = [\pi - \arccos(1/3)]J^{-1}/2$. Upon reinstating \hbar , the total Dicke-state preparation time within the framework of the proposed scheme is thus given by

$$T \approx 0.95 \frac{\hbar}{J}. \quad (18)$$

B. Realization with neutral-atom qubits

To examine the practical feasibility of this scheme, it is of interest to estimate the order of magnitude of the obtained state-preparation time in QC platforms of current interest. For instance, one promising platform is based on optically trapped neutral atoms confined in optical tweezers at a typical mutual distance of a few micrometers [57,80]. In such systems it is nowadays possible to prepare almost any two-dimensional arrangement of neutral atoms [78]; as a special case, one can prepare a system that consists of three equidistant neutral atoms. Assuming that the role of the logical qubit states $|0\rangle$ and $|1\rangle$ is played by the atomic ground state $|g\rangle$ and a high-lying Rydberg state $|r\rangle$ [77], respectively, such a system of three neutral-atom qubits is of direct relevance for the present work.

The Ising-type interaction between neutral-atom qubits originates from the vander Waals (vdW)-type interaction between atoms. This interaction is given by

$$\begin{aligned} V_{\text{vdW}} &= \sum_{n < n'} \frac{C_6}{R_{nn'}^6} |r_n r_{n'}\rangle \langle r_n r_{n'}| \\ &= \frac{1}{4} \sum_{n < n'} \frac{C_6}{R_{nn'}^6} (Z_n Z_{n'} + Z_n + Z_{n'} + 1), \end{aligned} \quad (19)$$

where $R_{nn'}$ is the distance between atoms n and n' and C_6 the vdW interaction constant. Thus, the Ising-coupling strength between Rydberg-atom qubits n and n' is given in this system by $J_{nn'} = C_6/(4R_{nn'}^6)$. For a typical interatomic distance of around $5 \mu\text{m}$ and a value around 50 for the principal quantum number [57] we have $J/\hbar \gtrsim 1.5\text{MHz}$. Therefore, based on Eq. (19) we find that $T \lesssim 0.6 \mu\text{s}$, which squares with the expectation that the time needed to carry out a typical entangling operation in such systems should be of the order of $1 \mu\text{s}$. The obtained state-preparation time is thus at least two orders of magnitude shorter than the typical radiative lifetimes of Rydberg states, which, for the chosen range of principal quantum numbers, are of the order of $100 \mu\text{s}$. This speaks in favor of the feasibility of the proposed scheme for the preparation of the state $|D_2^3\rangle$.

It is of interest to examine the feasibility of realizing the proposed state-preparation scheme with neutral-atom qubits in the presence of potentially debilitating effects such as motion-induced dephasing and ionization. In what follows, we demonstrate that under typical experimental conditions (such as the Lamb-Dicke regime of atomic motion and the presence of a cryogenic environment) these effects do not pose obstacles to the realization of the desired Dicke state in a system of neutral atoms confined in optical dipole traps (tweezers) [80].

Generally speaking, laser-based manipulation of atomic states gives rise to undesired phases that depend on atomic

positions. These effects are, however, alleviated when atoms are initially confined in the ground state of the trapping potential (in this particular case, that of an optical tweezer) and the system is in the Lamb-Dicke regime. This last case refers to situations where the trap is sufficiently confining that the momentum imparted by the scattered photon does not cause a change in the motional state of an atom [80]. In other words, the recoil energy of an atom is much smaller than the spacing between adjacent vibrational levels corresponding to the trapping potential.

Let us consider an atom of mass m whose position within a tweezer trap with frequency ω_{tr} is given by $x_n = x_n^0 + s_n$, where x_n^0 is its equilibrium position and $s_n = l_0(a_n + a_n^\dagger)$ the fluctuation due to its motion; here $l_0 \equiv \sqrt{\hbar/(2m\omega_{\text{tr}})}$ is the harmonic zero-point length corresponding to the motional ground state within a tweezer trap, while the creation (annihilation) operator a_n^\dagger (a_n) creates (destroys) a single excitation pertaining to the motional degrees of freedom of the considered atom. The atom is assumed to initially be in the state $|g\rangle_n|0\rangle_n \equiv |g, 0\rangle_n$, i.e., in the atomic ground state $|g\rangle$ and in the ground state $|0\rangle$ with respect to its motional degrees of freedom. The action of the Hamiltonian describing an atom-laser interaction on this state leads to the state $\Omega(t)e^{ikx_n}|e, 0\rangle_n$, where $\Omega(t)$ is the Rabi frequency of the external laser and $|e\rangle_n$ is an excited atomic state (one special case of such states is the Rydberg state $|r\rangle_n$). In the Lamb-Dicke regime, defined by the condition $\eta \equiv kl_0/\sqrt{2} \ll 1$, we can expand the exponential factor $e^{ikx_n} \equiv e^{ikx_n^0}e^{iks_n}$ and thereby obtain

$$e^{ikx_n} = e^{ikx_n^0}[1 + i\eta(a_n + a_n^\dagger) + O(\eta^2)]. \quad (20)$$

By first absorbing the constant prefactor $e^{ikx_n^0}$ into the definition of the atomic basis states, i.e., defining $|\tilde{e}\rangle_n \equiv e^{ikx_n^0}|e\rangle_n$, the Hamiltonian describing the laser-induced excitation of atom n in the basis $\{|g, 0\rangle_n, |\tilde{e}, 0\rangle_n, |\tilde{e}, 1\rangle_n\}$ adopts the form

$$H_{\text{exc}} = \begin{pmatrix} 0 & \Omega(t) & \eta\Omega(t) \\ \Omega(t) & 0 & 0 \\ \eta\Omega(t) & 0 & \omega_{\text{tr}} \end{pmatrix}. \quad (21)$$

If the considered atom starts in the state $|g, 0\rangle_n$, the probability of populating the state $|\tilde{e}, 1\rangle_n$ (a special case of $|\tilde{e}, 1\rangle_n$), which corresponds to the situation where the excitation of the considered atom to the desired Rydberg state is accompanied by the creation of a single motional quantum within the tweezer trap, will be negligible if $\Omega\eta \ll \omega_{\text{tr}}$. For a typical choice of parameter values of our envisioned system [$\Omega \sim 1\text{kHz}$, $\omega_{\text{tr}}/(2\pi) \sim (1-10)\text{kHz}$] being in the Lamb-Dicke regime ($\eta \ll 1$) immediately implies that this last condition is fulfilled. Therefore, the motion-induced dephasing does not have an appreciable detrimental impact on the realization of our state-preparation scheme.

Another possible source of decoherence in our envisioned neutral-atom system is depopulation of the Rydberg state. The rate of Rydberg-state depopulation is given by the sum of probabilities of spontaneous emission to all lower states, which are given by Einstein's coefficients A_{if} [77] (with $|i\rangle$

and $|f\rangle$ being the initial and final states, respectively)

$$\tau_r^{-1} = \sum_f A_{if} = \frac{2e^2}{3\epsilon_0 c^3 \hbar} \sum_{E_f < E_i} \omega_{if}^3 |\langle i|\mathbf{r}|f\rangle|^2. \quad (22)$$

Here $\omega_{if} \equiv (E_i - E_f)/\hbar$ is the transition frequency and $\langle i|\mathbf{r}|f\rangle$ the dipole matrix element between the initial and final states; importantly, the sum in Eq. (23) runs only over final states with energies smaller than that of the initial state. One of the possible Rydberg-decay channels corresponds to loss due to atomic collisions; however, such loss is heavily suppressed in the envisioned system because it is assumed that in this system there is only one atom in each individual tweezer trap. The other possible Rydberg-decay channel pertains to blackbody-radiation-induced transitions [77]. However, in a cryogenic environment, which the proposed system is assumed to operate in, such transitions are known to be negligible.

C. Geometric interpretation of the pulse sequence on the Bloch sphere

Making use of the permutational-symmetry of the state-engineering problem under consideration allows us to treat this problem in the four-dimensional symmetric sector (recall Sec. II C) rather than in the original, eight-dimensional Hilbert space of the three-qubit system. Further dimensional reduction of the problem at hand (to a two-dimensional space) is enabled through the decomposition of the relevant operators in the (two-dimensional) eigensubspaces of the x - and y -parity operators; the second of which are given by the tensor products of Pauli X and Y operators on different qubits

$$X_p \equiv X \otimes X \otimes X, \quad Y_p \equiv Y \otimes Y \otimes Y. \quad (23)$$

In what follows, we make use of this additional dimensional reduction to provide a geometric interpretation of the proposed pulse sequence on the Bloch sphere.

It is worthwhile to first note that the operators H_{ZZ} and $\mathcal{X} = X_1 + X_2 + X_3$ commute with the x -parity operator X_p (similarly, the operators H_{ZZ} and $\mathcal{Y} = Y_1 + Y_2 + Y_3$ commute with the y -parity operator Y_p). As a result, each of the two (degenerate) eigensubspaces of X_p , which correspond to the eigenvalues ± 1 , are invariant with respect to the operators H_{ZZ} and \mathcal{X} . This allows us to simplify the analysis of the dynamics inherent to H_{ZZ} and \mathcal{X} by projecting these operators to the $+1$ and -1 eigensubspaces of X_p .

While, generally speaking, the dimensionality of the $+1$ and -1 eigensubspaces of X_p is 4, in the problem at hand we are only interested in their corresponding eigenstates that belong to the symmetric sector (recall the discussion in Sec. II C). Thus, the relevant two-dimensional $+1$ eigensubspace of X_p is spanned by the states that in our chosen symmetric-sector basis [cf. Eq. (10)] are given by

$$|v_1\rangle = \frac{1}{\sqrt{2}} \begin{pmatrix} 1 \\ 0 \\ 0 \\ 1 \end{pmatrix}, \quad |v_2\rangle = \frac{1}{\sqrt{2}} \begin{pmatrix} 0 \\ 1 \\ 1 \\ 0 \end{pmatrix}, \quad (24)$$

while its -1 counterpart is spanned by

$$|v_3\rangle = \frac{1}{\sqrt{2}} \begin{pmatrix} 1 \\ 0 \\ 0 \\ -1 \end{pmatrix}, \quad |v_4\rangle = \frac{1}{\sqrt{2}} \begin{pmatrix} 0 \\ 1 \\ -1 \\ 0 \end{pmatrix}. \quad (25)$$

In the -1 eigensubspace of X_p the actions of H_{ZZ} and \mathcal{X} are represented, respectively, by the matrices

$$H_{ZZ}^{(-1)}/J = \begin{pmatrix} 3 & 0 \\ 0 & -1 \end{pmatrix}, \quad \mathcal{X}^{(-1)} = \begin{pmatrix} 0 & \sqrt{3} \\ \sqrt{3} & -2 \end{pmatrix}. \quad (26)$$

It is straightforward to express these 2×2 matrices in the basis $\{\mathbb{1}_2, X, Y, Z\}$,

$$H_{ZZ}^{(-1)}/J = \mathbb{1}_2 + 2Z, \\ \mathcal{X}^{(-1)} = -\mathbb{1}_2 + \sqrt{3}X + Z, \quad (27)$$

which can further be recast in the form

$$H_{ZZ}^{(-1)}/J = \mathbb{1}_2 + 2(0, 0, 1)^T \cdot \mathbf{X}, \\ \mathcal{X}^{(-1)} = -\mathbb{1}_2 + 2(\sqrt{3}/2, 0, 1/2)^T \cdot \mathbf{X}. \quad (28)$$

The form of the last equations implies that the time-evolution operators corresponding to the operators $H_{ZZ}^{(-1)}$ and $\mathcal{X}^{(-1)}$, acting in the -1 eigensubspace of X_p , have the form of global-rotation operators. Their respective rotation axes are defined by the unit vectors $(0, 0, 1)^T$ and $(\sqrt{3}/2, 0, 1/2)^T$.

The adopted initial state $|000\rangle$ of our state-preparation scheme is an equal-weight superposition of states in the $+1$ and -1 eigensubspaces of the parity operator, more precisely $|000\rangle = (|v_1\rangle + |v_3\rangle)/\sqrt{2}$. At the same time, the target state $|D_2^3\rangle$ is given by $|D_2^3\rangle = (|v_2\rangle - |v_4\rangle)/\sqrt{2}$.

The proposed five-stage pulse sequence, which gives rise to the state $|D_2^3\rangle$ starting from $|000\rangle$, consists of three global-rotation- and two Ising-interaction pulses, i.e.,

$$|D_2^3\rangle = U_C(\alpha_{3,0}, \phi_{3,0})U_{ZZ}(\xi_{2,0})U_C(\alpha_{2,0}, \phi_{2,0}) \\ \times U_{ZZ}(\xi_{1,0})U_C(\alpha_{1,0}, \phi_{1,0})|000\rangle, \quad (29)$$

where $\{\alpha_{1,0}, \alpha_{2,0}, \alpha_{3,0}, \phi_{1,0}, \phi_{2,0}, \phi_{3,0}, \xi_{1,0}, \xi_{2,0}\}$ are the optimal values of the pulse-sequence parameters given by Eq. (16). The last equation can straightforwardly be manipulated to the form

$$|D\rangle = U_{ZZ}(\xi_{2,0})U_C(\alpha_{2,0}, \phi_{2,0})U_{ZZ}(\xi_{1,0})|A\rangle, \quad (30)$$

where $|A\rangle = U_C(\alpha_{1,0}, \phi_{1,0})|000\rangle \equiv R_y(3\pi/2)|000\rangle$ is the state of the three-qubit system after the first global control pulse (a rotation around the y axis through an angle of $3\pi/2$) is carried out, while $|D\rangle = U_C^{-1}(\alpha_{3,0}, \phi_{3,0})|D_2^3\rangle \equiv R_y(-\pi/2)|D_2^3\rangle$ is its state before the third control pulse (a rotation around the y axis through an angle of $\pi/2$) is performed. In terms of the basis vectors $|v_3\rangle$ and $|v_4\rangle$ of the -1 eigensubspace of the x -parity operator X_p [cf. Eq. (26)], the states $|A\rangle$ and $|D\rangle$ are given by $|A\rangle = (\sqrt{3}|v_4\rangle - |v_3\rangle)/2$ and $|D\rangle = (\sqrt{3}|v_3\rangle + |v_4\rangle)/2$.

While the state $|000\rangle$, as explained above, represents a linear combination of states from two different eigensubspaces of X_p , the state $|A\rangle$ obtained from the second eigensubspace through the rotation $R_y(3\pi/2)$ belongs to the -1 eigensubspace. Because the same is true of the state $|D\rangle$, all three

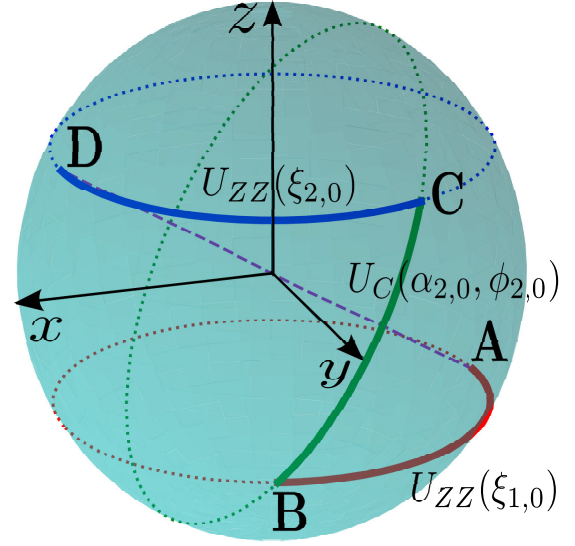


FIG. 2. Geometric interpretation of the proposed pulse sequence on the Bloch sphere, which pertains to the two-dimensional eigensubspace of the x -parity operator X_p that corresponds to the eigenvalue -1 . The point A on the Bloch sphere corresponds to the state $|A\rangle \equiv R_y(3\pi/2)|000\rangle$ of the system after the first global control pulse, while D pertains to its state $|D\rangle \equiv R_y(-\pi/2)|D_2^3\rangle$ before the third control pulse; the dashed line indicates the global-rotation axis corresponding to the operator $\mathcal{X}^{(-1)}$ in Eq. (29).

remaining stages of the pulse sequence [represented by the operators $U_{ZZ}(\xi_{1,0})$, $U_C(\alpha_{2,0}, \phi_{2,0})$, and $U_{ZZ}(\xi_{2,0})$ in Eq. (31)] lead to the evolution of the three-qubit system within that same (two-dimensional) eigensubspace of X_p . Given that it is confined to a two-dimensional subspace, this evolution can be visually represented using a Bloch sphere.

Before even attempting to provide a geometrical interpretation of the proposed pulse sequence, it is useful to recall that an arbitrary pure single-qubit state can be parametrized as [34]

$$|\Psi(\theta, \phi)\rangle = \cos \frac{\theta}{2} |0\rangle + e^{i\phi} \sin \frac{\theta}{2} |1\rangle, \quad (31)$$

where the values of the polar angle $\theta \in [0, \pi]$ and the azimuthal angle $\phi \in [0, 2\pi)$ define the point $(x, y, z) = (\sin \theta \cos \phi, \sin \theta \sin \phi, \cos \theta)$ that corresponds to the state $|\Psi(\theta, \phi)\rangle$ on the Bloch sphere. According to this parametrization, the north pole of the Bloch sphere ($\theta = 0$) corresponds to the logical $|0\rangle$ state, while the south pole ($\theta = \pi$) represents the state $|1\rangle$.

For our present purpose of geometrically representing unitary transformations in the relevant two-dimensional subspace of the original three-qubit Hilbert space, we choose the convention in which the eigenvector $|v_3\rangle$ is identified with the north pole of the Bloch sphere in Fig. 2 and $|v_4\rangle$ with the south pole [cf. Eq. (26)]. On this Bloch sphere the states $|A\rangle$ and $|D\rangle$ are represented by the eponymous points. At the same time, the three stages of the proposed pulse sequence that are required to steer the system from A to D are represented by following three curves: the curve A to B [the first Ising-interaction pulse, described by $U_{ZZ}(\xi_{1,0})$], B to C [the second control pulse, i.e., a rotation around the x axis through an angle of $-\arccos(1/3)/2$, represented by $U_C(\alpha_{2,0}, \phi_{2,0})$], and

C to D [the second Ising-interaction pulse; its corresponding time-evolution operator is $U_{ZZ}(\xi_{2,0})$]. All three curves have the same shape because in the relevant two-dimensional subspace of the original three-qubit Hilbert space both control pulses and their Ising-interaction counterparts act as global-rotation operators, as implied by the form of Eq. (29).

IV. ROBUSTNESS OF THE STATE-PREPARATION SCHEME

Having found the idealized pulse sequence for the preparation of the desired Dicke state [cf. Eq. (16) in Sec. III A], it is pertinent to quantitatively assess the sensitivity of the proposed state-preparation scheme to various imperfections. Typical imperfections considered in NMR-type pulse sequences [52] pertain to errors in the rotation axes (more precisely, in the directions of their corresponding unit vectors $\hat{\mathbf{n}}$) and/or errors in the rotation angles. Thus, the actual qubit rotation carried out experimentally is not the ideal one represented by $R_{\hat{\mathbf{n}}}(2\theta) \equiv \exp[-i\theta(\hat{\mathbf{n}} \cdot \mathbf{X})]$ [cf. Eq. (13)]. A realistic rotation is instead described by

$$\tilde{R}_{\hat{\mathbf{n}}}(2\theta) = \exp[-i\mathbf{f}(\theta, \hat{\mathbf{n}}) \cdot \mathbf{X}], \quad (32)$$

where the vector function $\mathbf{f}(\theta, \hat{\mathbf{n}})$ characterizes various types of systematic errors [52]. For example, the form $\mathbf{f}(\theta, \hat{\mathbf{n}}) = \theta(1 + \varepsilon_\theta)\hat{\mathbf{n}}$ of this vector function allows us to describe under and overrotation errors (for negative and positive values of ε_θ , respectively). On the other hand, by choosing this function to have the form $\mathbf{f}(\theta, \hat{\mathbf{n}}) = \theta(n_x \cos \varepsilon_\phi + n_y \sin \varepsilon_\phi, n_y \cos \varepsilon_\phi - n_x \sin \varepsilon_\phi, n_z)^T$ we can capture the error in the rotation axis [52] whose nominal direction is given by the unit vector $\hat{\mathbf{n}} \equiv (\cos \phi, \sin \phi, 0)^T$.

In keeping with the above general considerations, we investigate the robustness of the proposed scheme by taking into account systematic errors in the global-rotation angles corresponding to the three control pulses (i.e., errors in the values of the parameters α_1 , α_2 , and α_3), errors in the directions of the attendant rotation axes (i.e., errors in the parameters ϕ_1 , ϕ_2 , and ϕ_3), and, finally, errors corresponding to the durations of the Ising-interaction pulses (ξ_1 and ξ_2). In other words, we consider errors ε_p of either sign for each of the eight characteristic pulse-sequence parameters ($p = \xi_1, \xi_2, \alpha_1, \alpha_2, \alpha_3, \phi_1, \phi_2, \phi_3$):

$$\begin{aligned} \xi_i &= \xi_{i,0}(1 + \varepsilon_{\xi_i}) \quad (i = 1, 2), \\ \alpha_j &= \alpha_{j,0}(1 + \varepsilon_{\alpha_j}), \quad \phi_j = \phi_{j,0} + \varepsilon_{\phi_j} \quad (j = 1, 2, 3). \end{aligned} \quad (33)$$

In connection with the form of the last equation, it is important to stress that errors in the parameters ξ_1 , ξ_2 , α_1 , α_2 , and α_3 have the nature of relative errors, while for ϕ_1 , ϕ_2 , and ϕ_3 it is pertinent to consider absolute errors. In both cases, we assume the corresponding errors to vary between -0.1 and 0.1 .

The relative impacts on the target-state fidelity \mathcal{F}_D of the individual deviations ε_p from the respective optimal values of the eight relevant parameters in the problem at hand are depicted in Fig. 3, which shows the deviation of the fidelity from unity (i.e., the infidelity) $1 - \mathcal{F}_D$. What can be inferred from these results is that, among these eight parameters, the Dicke-state fidelity is by far most sensitive to deviations from the optimal value of the parameter α_1 , i.e., the global-rotation

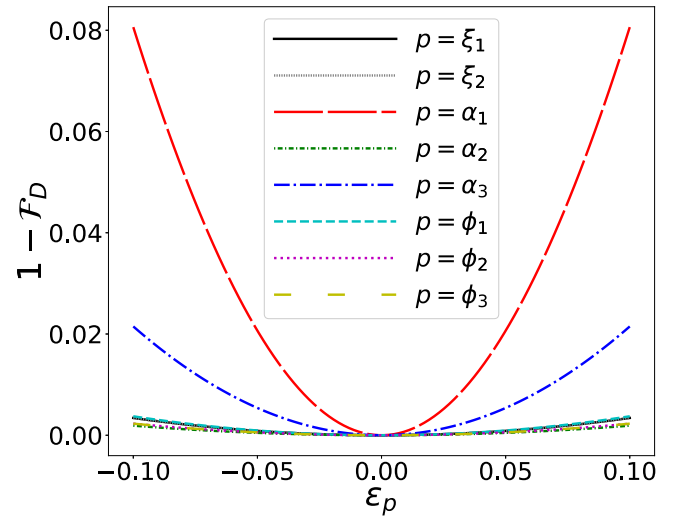


FIG. 3. Dependence of the deviation of the Dicke-state fidelity from unity $1 - \mathcal{F}_D$ on the errors ε_p in the values of the parameters that characterize the pulse sequence for implementing the Dicke-state preparation.

angle pertaining to the first ($t = 0$) control pulse. Another parameter whose variation significantly affects the target-state fidelity is α_3 , which determines the global-rotation angle corresponding to the third ($t = T$) control pulse. The errors in the values of the remaining six parameters have much smaller bearing on the target-state fidelity.

Apart from the impacts of deviations ε_p in the individual pulse-sequence parameters on the resulting Dicke-state fidelity, as illustrated by Fig. 3, it is pertinent to also quantitatively analyze the effect of simultaneous errors in more than one pulse-sequence parameter. To achieve that, we numerically evaluated the fidelity \mathcal{F}_D in the presence of simultaneous errors in two different parameters, based on its defining expression [cf. Eq. (15)]. The results obtained in this manner for the infidelity $1 - \mathcal{F}_D$ are presented in the form of two-dimensional density plots in Figs. 4–7. The near-elliptical shape of different regions in these plots originates from the fact that the dependence of $1 - \mathcal{F}_D$ on the errors ε_p is to leading order quadratic because these errors represent deviations from the optimal parameter values.

For instance, Fig. 4(a) shows the deviation $1 - \mathcal{F}_D$ of the fidelity from unity in the presence of simultaneous errors in the parameters α_1 and α_2 . Apart from corroborating the aforementioned conclusion that the target-state fidelity is much more sensitive to the deviation in the first rotation angle (α_1) than in the second one (α_2), another interesting quantitative insight can be gleaned from this density plot. Namely, it can be inferred from this plot that, as long as the relative errors in these two parameters are below 5%, the infidelity $1 - \mathcal{F}_D$ does not exceed 2%, i.e., the Dicke-state fidelity is at least 0.98.

Figure 4(b) illustrates the dependence of the infidelity on the deviations from the optimal values of the parameters ϕ_1 and ϕ_2 . What is immediately noticeable from this density plot is that the relevant infidelities are, roughly speaking, an order of magnitude lower than in the previously considered case of α_1 and α_2 [cf. Fig. 4(a)]. For instance, with the exception of very large deviations of ϕ_1 and ϕ_2 in the same direction (i.e.,

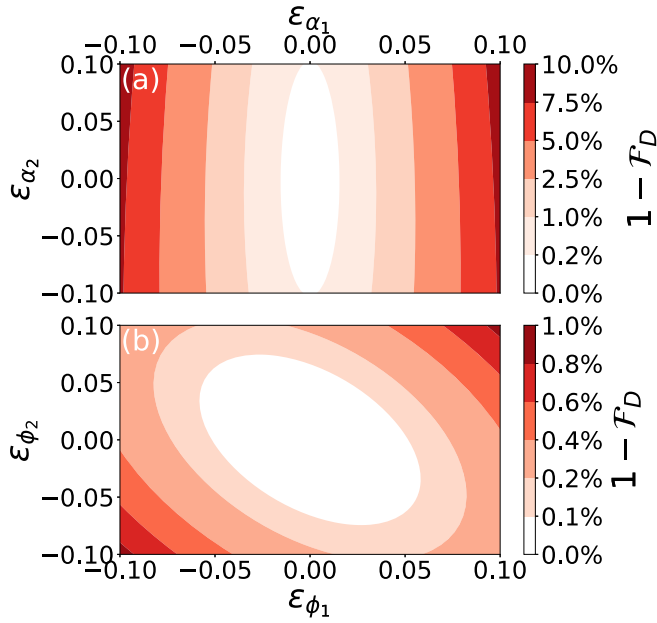


FIG. 4. Dependence of the deviation $1 - \mathcal{F}_D$ of the Dicke-state fidelity from unity on (a) errors in the parameters α_1 and α_2 , i.e. deviations from their respective optimal values $\alpha_{1,0} = 3\pi/4$ and $\alpha_{2,0} = -\arccos(1/3)/4$, and (b) errors in the parameters ϕ_1 and ϕ_2 , i.e. deviations from their respective optimal values $\phi_{1,0} = \pi/2$ and $\phi_{2,0} = 0$.

ε_{ϕ_1} and ε_{ϕ_2} have the same sign), the infidelity does not exceed 0.8%; in other words, the Dicke-state fidelity is above 0.99 in almost the entire range of errors discussed. An important qualitative observation is that, in contrast to the dependence of the infidelity on errors in the last two parameters, which is

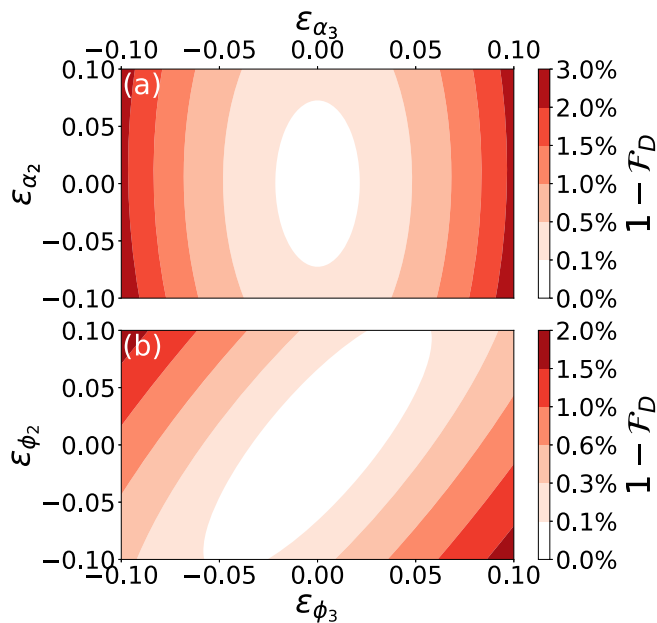


FIG. 5. Dependence of the deviation $1 - \mathcal{F}_D$ of the Dicke-state fidelity from unity on (a) errors in the parameters α_2 and α_3 , i.e. deviations from their respective optimal values $\alpha_{2,0} = -\arccos(1/3)/4$ and $\alpha_{3,0} = \pi/4$, and (b) errors in the parameters ϕ_2 and ϕ_3 , i.e. deviations from their respective optimal values $\phi_{2,0} = 0$ and $\phi_{3,0} = \pi/2$.

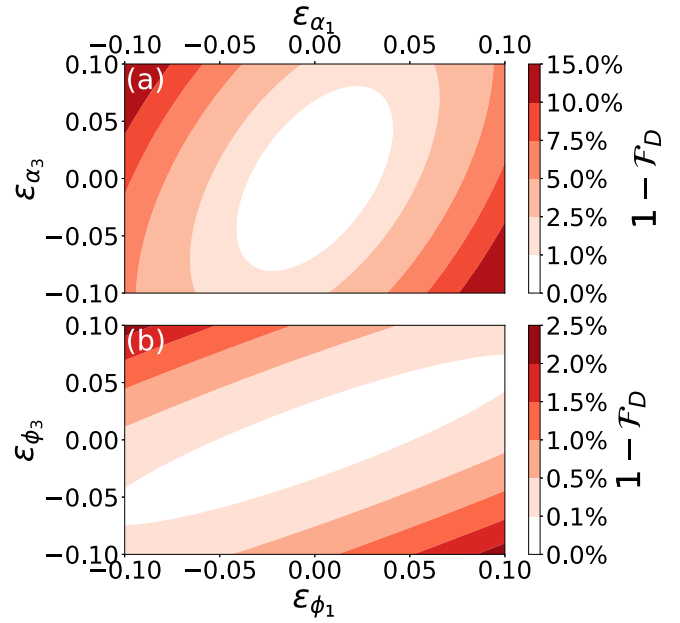


FIG. 6. Dependence of the deviation $1 - \mathcal{F}_D$ of the Dicke-state fidelity from unity on (a) errors in the parameters α_1 and α_3 , i.e. deviations from their respective optimal values $\alpha_{1,0} = 3\pi/4$ and $\alpha_{3,0} = \pi/4$, and (b) errors in the parameters ϕ_1 and ϕ_3 , i.e. deviations from their optimal values $\phi_{1,0} = \phi_{3,0} = \pi/2$.

completely symmetric with respect to the change of their sign, the dependence of $1 - \mathcal{F}_D$ on ε_{ϕ_1} and ε_{ϕ_2} is highly asymmetric with respect to such a change of sign.

The dependence of the infidelity on the errors in the parameters α_2 and α_3 , which is illustrated in Fig. 5(a), is qualitatively similar to that of α_1 and α_2 [cf. Fig. 4(a)]. The main quantitative difference is that the elliptical regions in Fig. 5(a) are somewhat less elongated along the ε_{α_2} axis than their counterparts in Fig. 4(a). In other words, the aspect ratio of the relevant elliptical curves is smaller than in Fig. 4(a), which is yet another reflection of the dominant role of errors in the parameter α_1 compared to errors in other pulse-sequence

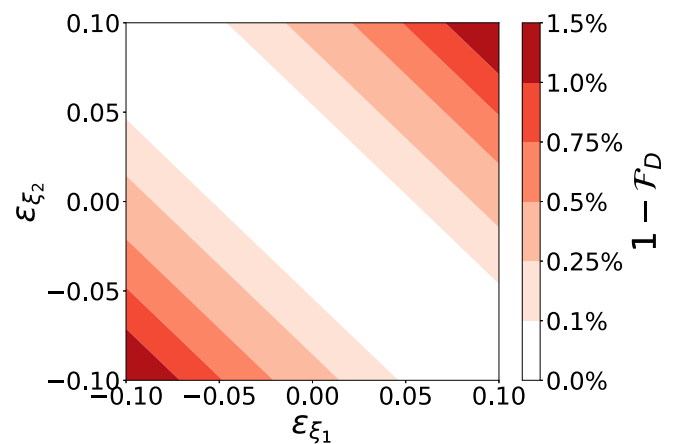


FIG. 7. Dependence of the deviation $1 - \mathcal{F}_D$ of the Dicke-state fidelity from unity on errors in the Ising-pulse durations ξ_1 and ξ_2 , i.e. deviations from their optimal values $\xi_{1,0} = \xi_{2,0} = [\pi - \arccos(1/3)]/4$.

parameters. This trend is also evident in Fig. 6(a), where the effect of simultaneous errors in the parameters α_1 and α_3 is illustrated. Another effect noticeable in the case of the later pair of parameters is the tilted orientation of the elliptical regions.

Figure 5(b) illustrates the dependence of the infidelity $1 - \mathcal{F}_D$ on the simultaneous errors in the parameters ϕ_2 and ϕ_3 , while Fig. 6(b) depicts a similar dependence on the errors in ϕ_1 and ϕ_3 . Compared to Fig. 4(b) the relevant infidelities are somewhat larger in the latter two cases. However, the target-state fidelities are still very close to unity (more precisely, higher than 0.98 and 0.975, respectively) even for the largest considered values of errors in those parameters. This speaks in favor of the robustness of the proposed state-preparation scheme.

In contrast to the rotation angles $\alpha_1, \alpha_2, \alpha_3$, the simultaneous errors in the parameters ϕ_1, ϕ_2, ϕ_3 exhibit elliptical regions that are mainly elongated in the diagonal and antidiagonal directions. To provide a plausible explanation for this observation, we note that the entire system is axially symmetric, i.e., invariant under rotations around the z axis. More precisely, the x and y axes can be chosen arbitrarily and a rotation around the z axis merely leads to a physically irrelevant complex phase of the Dicke state. In particular, the Dicke-state fidelity ought to be invariant under uniform translations, i.e., transformations $\phi_1, \phi_2, \phi_3 \mapsto \phi_1 + \epsilon, \phi_2 + \epsilon, \phi_3 + \epsilon$ for an arbitrary $\epsilon \in \mathbb{R}$. Needless to say, this invariance is not borne out by the obtained results as they correspond to the case of two simultaneous errors instead of three. However, this invariance makes the predominant orientation of the elliptical regions in the diagonal and antidiagonal directions plausible. For instance, the aforementioned symmetry implies that an error in the diagonal direction, that is, the same errors in two angles (e.g., $\phi_{0,1}, \phi_{0,2} + \epsilon, \phi_{0,3} + \epsilon$), coincides with an error in the third angle (e.g., $\phi_{0,1} - \epsilon, \phi_{0,2}, \phi_{0,3}$). This last observation allows us to compare simultaneous errors in two angles ϕ_i and ϕ_j in the diagonal direction to an error in the remaining angle ϕ_k ($i, j, k = 1, 2, 3$). In particular, Fig. 3 shows that the fidelity is most sensitive to deviations in ϕ_3 (up to around 0.9%). This matches with the elliptical regions pertaining to deviations in ϕ_1 and ϕ_2 in Fig. 4(b), which are oriented in the antidiagonal direction; thus, the fastest increase of the infidelity is the one in the diagonal direction (also up to about 0.9%). Conversely, the elliptical regions corresponding to deviations in (ϕ_1, ϕ_3) and (ϕ_2, ϕ_3) in Figs. 5(b) and 6(b) are tilted in the diagonal direction, which corresponds to deviations in ϕ_2 and ϕ_1 , respectively. Consistently, the infidelity increases more slowly in the diagonal direction than along the ϕ_3 axis.

As can be inferred from Fig. 7, the fidelity appears to remain equal to unity for antidiagonal errors in ξ_1 and ξ_2 , i.e., for $\xi_1 = \xi_{1,0} + \epsilon$ and $\xi_2 = \xi_{2,0} - \epsilon$ for $\epsilon \in \mathbb{R}$. This somewhat surprising observation should, however, be taken with caution because the fidelity does, in fact, deviate from unity for antidiagonal errors, even if this deviation is hardly noticeable. Notwithstanding, we note that this observation is physically reasonable given that the total duration T of the pulse sequence remains invariant under antidiagonal errors in ξ_1 and ξ_2 , this being a consequence of the fact that the total duration is proportional to $\xi_1 + \xi_2$.

V. GENERALIZATION: DICKE-STATE PREPARATION FOR $N \geq 4$

For the sake of completeness, it is worthwhile to explain how the proposed scheme for the generation of the state $|D_2^3\rangle$ can be generalized to other Dicke states, in particular in systems with $N \geq 4$ qubits. To this end, we start this section with some general, permutational-symmetry related considerations (Sec. V A). We then present the resulting pulse sequence for realizing the two-excitation Dicke state in a four-qubit system, i.e., the state $|D_2^4\rangle$ (Sec. V B).

A. General permutational-symmetry-based considerations

To begin with, it is worthwhile to note that in an N -qubit system the subspace of permutationally invariant states corresponds to the total spin of $N/2$; the simplest example is furnished by the $N = 2$ case, i.e., that of two spin-1/2 particles, where the permutationally invariant subspace corresponds to the total spin of 1 and is three-dimensional (the spin-triplet subspace). Accordingly, the dimension of this permutationally invariant subspace is equal to $N + 1$ [81], hence increasing linearly with the number of qubits. This very fact [that the dimension of the relevant permutationally invariant subspace grows only linearly, and that of the total Hilbert space exponentially (i.e., as 2^N), with the number of qubits] speaks in favor of exploiting the permutational symmetry in the context of quantum-state engineering in systems of this type.

One commonly used complete orthonormal basis of the permutationally invariant subspace of the N -qubit Hilbert space is given by the Dicke states $|D_a^N\rangle$ ($a = 0, \dots, N$) [cf. Eq. (5)]. In other words, any permutationally invariant state of N qubits can be expressed as a linear combination of the $N + 1$ states of this symmetry-adapted basis; as a reminder, the basis in Eq. (10) is the special $N = 3$ case of this general Dicke-state basis.

For an arbitrary qubit number N , it is straightforward to obtain the matrices representing the time-evolution operators $U_{ZZ}(\xi_j)$ and $U_C(\alpha_j)$ in the chosen symmetry-adapted (Dicke-state) basis. To derive the matrix form of $U_{ZZ}(\xi_j)$, we first note that H_{ZZ} is diagonal for each value of N . The corresponding matrix elements of H_{ZZ} are given by

$$\langle D_a^N | H_{ZZ} | D_a^N \rangle = 2 \left(a - \frac{N}{2} \right)^2 - \frac{N}{2}, \quad (34)$$

where $a = 0, \dots, N$. Hence, a simple matrix exponentiation yields

$$\langle D_a^N | U_{ZZ}(\xi_j) | D_a^N \rangle = e^{-i\xi_j [2(a-N/2)^2 - N/2]}. \quad (35)$$

On the other hand, the time-evolution operator $U_C(\alpha_j)$ corresponding to the j th control pulse ($j = 1, 2, \dots$) is given by

$$U_C(\alpha_j) = e^{-i\alpha_j \mathcal{S}_1^{(j)}}, \quad (36)$$

where the operator $\mathcal{S}_1^{(j)}$ is defined as [cf. Eq. (3)]

$$\mathcal{S}_1^{(j)} = \cos \phi_j \mathcal{X} + \sin \phi_j \mathcal{Y}. \quad (37)$$

It is straightforward to demonstrate that the matrix elements of $\mathcal{S}_1^{(j)}$ in the Dicke-state basis are given by

$$\begin{aligned} \langle D_a^N | \mathcal{S}_1^{(j)} | D_b^N \rangle &= (\delta_{b,a+1} e^{i\phi_j} + \delta_{b,a-1} e^{-i\phi_j}) \\ &\times \sqrt{\frac{b+a+1}{2} \left(N - \frac{b+a-1}{2} \right)}, \end{aligned} \quad (38)$$

for $a, b = 0, \dots, N$. Because $\mathcal{S}_1^{(j)}$ is not diagonal in the chosen basis, one can compute $U_C(\alpha_j)$ using matrix exponentiation, which even in the most general case can efficiently be carried out numerically.

Further insight into the problem of generating Dicke states in the N -qubit case can be gleaned by noting that the operators H_{ZZ} and \mathcal{X} commute with the x -parity operator $X_p \equiv X \otimes X \otimes \dots \otimes X$. Consequently, these two operators can be block-diagonalized in the two eigensubspaces of X_p that correspond to the eigenvalues ± 1 ; the bases of these two eigensubspaces of X_p are given by

$$|v_k^\pm\rangle = c_k (|D_{k-1}^N\rangle \pm |D_{N-k+1}^N\rangle), \quad (39)$$

where c_k is the normalization constant and $k = 1, \dots, \lfloor N/2 \rfloor + 1$ (where, for a real number x , $\lfloor x \rfloor$ is the largest integer not larger than x). Note that for even values of N and the corresponding values of k such that the two subscripts of Dicke states in Eq. (40) are the same [i.e., for $N = 2(k-1)$] the basis vector $|v_k^-\rangle$ vanishes; therefore, in that case the $+1$ and -1 eigensubspaces of the $(N+1)$ -dimensional permutationally invariant subspace of the total N -qubit Hilbert space have dimensions equal to $1 + N/2$ and $N/2$, respectively.

Similarly, the operators H_{ZZ} and \mathcal{Y} commute with the y -parity operator $Y_p \equiv Y \otimes Y \otimes \dots \otimes Y$ and, as a result, can both be block-diagonalized in the ± 1 eigensubspaces of Y_p . The respective bases of these two eigensubspaces of Y_p are given by

$$|w_k^\pm\rangle = c_k [|D_{k-1}^N\rangle \pm i^N (-1)^k |D_{N-k+1}^N\rangle], \quad (40)$$

where c_k and k have the same meaning as in Eq. (40) above.

B. Pulse sequence for realizing the state $|D_2^4\rangle$

Having discussed permutational-symmetry-related aspects of the Dicke-state preparation in an N -qubit system in Sec. V A, we now proceed to illustrate this general approach on the example of the two-excitation Dicke state in a four-qubit system, i.e., the state $|D_2^4\rangle$. As we demonstrate in what follows, similar to the case of $|D_2^3\rangle$ the state $|D_2^4\rangle$ can also be realized starting from the state $|0000\rangle$ through a pulse sequence that consists of three global-control pulses and two Ising-interaction pulses, i.e., a pulse sequence of the type illustrated in Fig. 1.

In the four-qubit case ($N = 4$), the five relevant permutationally invariant basis states are $|D_0^4\rangle \equiv |0000\rangle$, $|D_1^4\rangle$, $|D_2^4\rangle$, $|D_3^4\rangle$, and $|D_4^4\rangle \equiv |1111\rangle$ [for the explicit form of these states, see Eq. (A12)].

To determine the optimal values of the pulse-sequence parameters, we optimize the target-state fidelity, which is given by an analog of Eq. (15). Namely, this state fidelity in the

four-qubit case is given by

$$\mathcal{F}_D = \langle |D_2^4\rangle | \mathcal{U}_{\text{PS}}(\xi_1, \xi_2, \alpha_1, \alpha_2, \alpha_3) | 0000 \rangle. \quad (41)$$

The optimal values of the eight pulse-sequence parameters, obtained numerically using the method previously employed in the three-qubit case (cf. Sec. III A) are

$$\begin{aligned} \alpha_{1,0} &= \pi/4, & \alpha_{2,0} &= -1.162, & \alpha_{3,0} &= -2.484, \\ \phi_{1,0} &= \pi/2, & \phi_{2,0} &= \phi_{3,0} = 0, \\ \xi_{1,0} &= 0.285, & \xi_{2,0} &= 0.702. \end{aligned} \quad (42)$$

Based on the obtained optimal parameter values we can conclude that the total duration $T = (\xi_{1,0} + \xi_{2,0}) J^{-1}$ of the pulse sequence for realizing the state $|D_2^4\rangle$ is (upon reinstating \hbar) given by $T \approx 0.99 \hbar/J$, which is just slightly longer than the time needed to realize the state $|D_2^3\rangle$ [cf. Eq. (19)]. Another, qualitative difference from the pulse sequence used for the preparation of $|D_2^3\rangle$ [cf. Sec. III A] is that in the four-qubit case the two Ising-interaction pulses do not have equal durations (i.e., $\xi_{1,0} \neq \xi_{2,0}$).

The obtained optimal values of the parameters α_j and ϕ_j ($j = 1, 2, 3$) can be made plausible through the following algebraic analysis. To begin with, we recall that the operators H_{ZZ} and \mathcal{X} commute with the parity operator X_p , implying that the eigensubspaces of X_p are invariant under the action of H_{ZZ} and \mathcal{X} (cf. Sec. V A). The eigensubspaces of X_p corresponding to the eigenvalues $+1$ and -1 are spanned by the vectors $\{|v_1^+\rangle, |v_2^+\rangle, |v_3^+\rangle\}$ and $\{|v_1^-\rangle, |v_2^-\rangle\}$, respectively, where [cf. Eq. (40)]

$$|v_1^\pm\rangle = \frac{1}{\sqrt{2}} \begin{pmatrix} 1 \\ 0 \\ 0 \\ 0 \end{pmatrix}, \quad |v_2^\pm\rangle = \frac{1}{\sqrt{2}} \begin{pmatrix} 0 \\ 1 \\ 0 \\ \pm 1 \end{pmatrix}, \quad |v_3^+\rangle = \begin{pmatrix} 0 \\ 0 \\ 1 \\ 0 \\ 0 \end{pmatrix}. \quad (43)$$

In keeping with the general conclusion stated in Sec. V A above, the respective dimensions of the $+1$ and -1 eigensubspaces of X_p are 3 and 2.

It is straightforward to first verify that $|D_2^4\rangle = |v_3^+\rangle$, i.e., the target state of our state-preparation scheme belongs to the subspace spanned by the vectors $\{|v_1^+\rangle, |v_2^+\rangle, |v_3^+\rangle\}$. Therefore, it suffices to first convert the initial state $|0000\rangle \equiv |D_0^4\rangle$ into a state that belongs to this last subspace, thereby effectively reducing the state-preparation problem at hand to the same subspace. It turns out that the desired initial-state conversion requires a control pulse $U_C(\alpha_{1,0}) \equiv U_C(\alpha_{1,0}, \phi_{1,0})$ with $\alpha_{1,0} = \pi/4$ and $\phi_{1,0} = \pi/2$, which corresponds to a rotation through an angle of $\pi/2$ around the y axis. By first expressing $U_C(\alpha_{1,0} = \pi/4, \phi_{1,0} = \pi/2)$ in the symmetry-adapted basis, by means of Eq. (A15), we obtain

$$U_C(\alpha_{1,0}) |D_0^4\rangle = \frac{1}{4} \begin{pmatrix} 1 \\ 2 \\ \sqrt{6} \\ 2 \\ 1 \end{pmatrix} = \frac{|v_1^+\rangle + 2|v_2^+\rangle + \sqrt{3}|v_3^+\rangle}{2\sqrt{2}}. \quad (44)$$

This allows us to reduce the subsequent control pulses $U_C(\alpha_{2,0})$ and $U_C(\alpha_{3,0})$ to the subspace spanned by

$\{|v_1^+\rangle, |v_2^+\rangle, |v_3^+\rangle\}$, which reveals that these control pulses correspond to global rotations around the x axis, i.e., $\phi_{2,0} = \phi_{3,0} = 0$. The remaining optimization problem, i.e., the maximization of the state fidelity in Eq. (42) with respect to the remaining four pulse-sequence parameters, leading to the results given by Eq. (43), can also be reduced by projecting the operators H_{ZZ} and \mathcal{X} into the same subspace:

$$H_{ZZ} \mapsto J \begin{pmatrix} 6 & 0 & 0 \\ 0 & 0 & 0 \\ 0 & 0 & -2 \end{pmatrix}, \quad \mathcal{X} \mapsto 2 \begin{pmatrix} 0 & 1 & 0 \\ 1 & 0 & \sqrt{3} \\ 0 & \sqrt{3} & 0 \end{pmatrix}. \quad (45)$$

VI. SUMMARY AND CONCLUSION

In summary, in this paper we addressed the problem of deterministically preparing the two-excitation Dicke state in a system that consists of three all-to-all Ising-coupled qubits acted upon by global control fields in the transverse directions. This system is state-to-state controllable for an arbitrary pair of initial and final states that are invariant with respect to permutations of qubits [60]. The permutational invariance of the Dicke state allowed us to carry out our analysis within the four-dimensional subspace of the three-qubit Hilbert space that consists of such (permutationally invariant) states.

We found a solution of the Dicke-state preparation problem that has the form of a five-stage NMR-type pulse sequence, which comprises three instantaneous control pulses (equivalent to global qubit rotations) and two Ising-interaction pulses. Through numerical optimization of the Dicke-state fidelity, we determined the optimal values of the eight parameters characterizing the envisioned pulse sequence. We then investigated the robustness of the proposed pulse sequence to systematic errors, i.e., deviations from the optimal values of those parameters. Importantly, we demonstrated that the Dicke-state fidelity remained very close to unity even for fairly large deviations from the optimal values of the relevant pulse-sequence parameters.

We also explained how our proposed scheme for the preparation of Dicke states can be generalized to systems with $N \geq 4$ qubits, describing, as an example, the preparation of the two-excitation Dicke state $|D_2^4\rangle$ in a four-qubit system. Likewise, the preparation of Dicke states could be addressed for qubit arrays with other relevant types of qubit-qubit interaction; for example, one could investigate this problem for an XY -type interaction, which is characteristic of superconducting qubits [82–85], as well as for Heisenberg-type interactions that are of relevance for spin qubits [86–88]. Experimental realization of the proposed state-preparation scheme in a physical platform with Ising-type coupling between qubits is keenly anticipated.

ACKNOWLEDGMENTS

This research was supported by the Deutsche Forschungsgemeinschaft (DFG) – SFB 1119 – 236615297.

APPENDIX: DERIVATION OF THE RELEVANT TIME-EVOLUTION OPERATORS

In the following, we sketch the derivation of the time-evolution operators corresponding to the control- and

Ising-interaction pulses required for the preparation of the Dicke state $|D_2^3\rangle$ in a three-qubit ($N = 3$) system (see Sec. A 1 below), as well as its counterpart $|D_2^4\rangle$ in a four-qubit ($N = 4$) one (Sec. A 2).

1. $N = 3$ case

We start by representing the Ising-interaction Hamiltonian of a three-qubit ($N = 3$) system [cf. Eq. (7)] in the symmetry-adapted basis of Eq. (11):

$$H_{ZZ} \mapsto J \begin{pmatrix} 3 & 0 & 0 & 0 \\ 0 & -1 & 0 & 0 \\ 0 & 0 & -1 & 0 \\ 0 & 0 & 0 & 3 \end{pmatrix}. \quad (A1)$$

Given that H_{ZZ} is already diagonal in the chosen basis, it is straightforward to write the explicit form of the time-evolution operators $U_{ZZ}(\xi_i)$ corresponding to both Ising interaction pulses ($i = 1, 2$). Namely, these time-evolution operators are given by

$$U_{ZZ}(\xi_i) = e^{-i\xi_i H_{ZZ}/J} \mapsto \begin{pmatrix} e^{-3i\xi_i} & 0 & 0 & 0 \\ 0 & e^{i\xi_i} & 0 & 0 \\ 0 & 0 & e^{i\xi_i} & 0 \\ 0 & 0 & 0 & e^{-3i\xi_i} \end{pmatrix}, \quad (A2)$$

with $\xi_1 \equiv JT_m$ being the dimensionless duration of the first interaction pulse and $\xi_2 \equiv J(T - T_m)$ that of the second one.

We now turn to the derivation of the time-evolution operators $U_C(\alpha_j)$ corresponding to the three instantaneous global control pulses ($j = 1, 2, 3$) [cf. Eq. (12)]. It is pertinent to first note that, while the corresponding (time-dependent) control Hamiltonian [cf. Eq. (8)] involves the mutually noncommuting Pauli operators X_n and Y_n of the n th qubit ($n = 1, 2, 3$), the x and y control fields have the same time dependence. As a result, this control Hamiltonian commutes with itself at different times (i.e., $[H_C(t), H_C(t')] = 0$). Accordingly, its corresponding time-evolution operator can be written in the simple form $\exp[-i \int_{t_i}^{t_f} H_C(t) dt]$ (with t_i and t_f being the initial and final evolution times, respectively), rather than assuming the most general form of a time-ordered exponential. More specifically yet, this time-evolution operator has the form of an exponential of a linear combination of the Pauli operators X_n and Y_n ($n = 1, 2, 3$).

By making use of the identity in Eq. (13), we arrive at the following expression for $U_C(\alpha_j)$ ($j = 1, 2, 3$):

$$U_C(\alpha_j) = \prod_{n=1}^3 [\cos \alpha_j \mathbb{1}_8 - i \sin \alpha_j \mathcal{A}_n^{(j)}]. \quad (A3)$$

The operators $\mathcal{A}_n^{(j)}$ ($n = 1, 2, 3$) are here defined as

$$\mathcal{A}_n^{(j)} = \frac{1}{\alpha_j} (\alpha_{j,x} X_n + \alpha_{j,y} Y_n), \quad (A4)$$

where $\alpha_j \equiv \|\alpha_j\| > 0$ is the norm of the vector α_j , while $\alpha_{j,x}$ and $\alpha_{j,y}$ are its x and y components, respectively. The form of Eq. (A3), in conjunction with that of Eq. (A4), makes it manifest that the three instantaneous global control pulses are equivalent to global qubit rotations.

To obtain an explicit form of the time-evolution operators $U_C(\alpha_j)$, we proceed by performing the following two steps.

First, it should be noted that, using the polar coordinates in the x - y plane the operator $\mathcal{A}_n^{(j)}$, acting on qubit n , can be recast in a simpler form. This is based on the identity

$$\frac{1}{\alpha_j} (\alpha_{j,x} X + \alpha_{j,y} Y) = \begin{pmatrix} 0 & e^{-i\phi_j} \\ e^{i\phi_j} & 0 \end{pmatrix} \quad (\text{A5})$$

for single-qubit Pauli operators, with ϕ_j being the polar angle corresponding to the vector α_j . Second, by carrying out the multiplication in Eq. (A3) we obtain the expression

$$U_C(\alpha_j) = \cos^3 \alpha_j \mathbb{1}_8 - i \sin \alpha_j \cos^2 \alpha_j \mathcal{S}_1^{(j)} - \sin^2 \alpha_j \cos \alpha_j \mathcal{S}_2^{(j)} + i \sin^3 \alpha_j \mathcal{S}_3^{(j)}, \quad (\text{A6})$$

for $U_C(\alpha_j)$, where the auxiliary operators $\mathcal{S}_1^{(j)}$, $\mathcal{S}_2^{(j)}$, and $\mathcal{S}_3^{(j)}$ ($j = 1, 2, 3$) are obtained from $\mathcal{A}_n^{(j)}$ ($n = 1, 2, 3$) using the following formulas:

$$\begin{aligned} \mathcal{S}_1^{(j)} &= \sum_{n=1}^3 \mathcal{A}_n^{(j)}, \\ \mathcal{S}_2^{(j)} &= \sum_{n < n'} \mathcal{A}_n^{(j)} \mathcal{A}_{n'}^{(j)}, \\ \mathcal{S}_3^{(j)} &= \prod_{n=1}^3 \mathcal{A}_n^{(j)}. \end{aligned} \quad (\text{A7})$$

When represented in the symmetry-adapted basis of Eq. (11), these operators are given by the 4×4 matrices

$$\begin{aligned} P_S \mathcal{S}_0^{(j)} P_S^\dagger &= \mathbb{1}_4, \\ P_S \mathcal{S}_1^{(j)} P_S^\dagger &= \begin{pmatrix} 0 & \sqrt{3} e^{-i\phi_j} & 0 & 0 \\ \sqrt{3} e^{i\phi_j} & 0 & 2e^{-i\phi_j} & 0 \\ 0 & 2e^{i\phi_j} & 0 & \sqrt{3} e^{-i\phi_j} \\ 0 & 0 & \sqrt{3} e^{i\phi_j} & 0 \end{pmatrix}, \\ P_S \mathcal{S}_2^{(j)} P_S^\dagger &= \begin{pmatrix} 0 & 0 & \sqrt{3} e^{-2i\phi_j} & 0 \\ 0 & 2 & 0 & \sqrt{3} e^{-2i\phi_j} \\ \sqrt{3} e^{2i\phi_j} & 0 & 2 & 0 \\ 0 & \sqrt{3} e^{2i\phi_j} & 0 & 0 \end{pmatrix}, \\ P_S \mathcal{S}_3^{(j)} P_S^\dagger &= \begin{pmatrix} 0 & 0 & 0 & e^{-3i\phi_j} \\ 0 & 0 & e^{-i\phi_j} & 0 \\ 0 & e^{i\phi_j} & 0 & 0 \\ e^{3i\phi_j} & 0 & 0 & 0 \end{pmatrix}, \end{aligned} \quad (\text{A8})$$

where P_S denotes the projector onto the symmetric sector [cf. Sec. II C]. By inserting these last matrices into Eq. (A6), after elementary manipulations we can obtain the matrices representing the time-evolution operators $U_C(\alpha_j)$ in the chosen basis. The rather cumbersome final expressions will, however, not be provided explicitly here.

2. $N = 4$ case

Having presented a detailed derivation of the relevant time-evolution operators for a three-qubit system (cf. Sec. A 1), in what follows we briefly sketch the derivation of their four-qubit ($N = 4$) counterparts.

In the $N = 4$ case the five (permutationally invariant) Dicke basis states [cf. Eq. (5)] are given by

$$\begin{aligned} |D_0^4\rangle &\equiv |0000\rangle, \\ |D_1^4\rangle &\equiv \frac{1}{2} (|1000\rangle + |0100\rangle + |0010\rangle + |0001\rangle), \\ |D_2^4\rangle &\equiv \frac{1}{\sqrt{6}} (|1100\rangle + |1010\rangle + |1001\rangle \\ &\quad + |0110\rangle + |0101\rangle + |0011\rangle), \\ |D_3^4\rangle &\equiv \frac{1}{2} (|1110\rangle + |1101\rangle + |1011\rangle + |0111\rangle), \\ |D_4^4\rangle &\equiv |1111\rangle. \end{aligned} \quad (\text{A9})$$

By first performing a mapping of these basis states onto column vectors, by analogy to Eq. (11), the Ising-interaction Hamiltonian of a four-qubit system is represented in the last symmetry-adapted basis as

$$H_{ZZ} \mapsto J \begin{pmatrix} 6 & 0 & 0 & 0 & 0 \\ 0 & 0 & 0 & 0 & 0 \\ 0 & 0 & -2 & 0 & 0 \\ 0 & 0 & 0 & 0 & 0 \\ 0 & 0 & 0 & 0 & 6 \end{pmatrix}. \quad (\text{A10})$$

The form of the last equation directly leads us to conclude that the corresponding time-evolution operators $U_{ZZ}(\xi_i)$ ($i = 1, 2$) are given by

$$U_{ZZ}(\xi_i) = e^{-i\xi_i H_{ZZ}/J} \mapsto \begin{pmatrix} e^{-6i\xi_i} & 0 & 0 & 0 & 0 \\ 0 & 1 & 0 & 0 & 0 \\ 0 & 0 & e^{2i\xi_i} & 0 & 0 \\ 0 & 0 & 0 & 1 & 0 \\ 0 & 0 & 0 & 0 & e^{-6i\xi_i} \end{pmatrix}. \quad (\text{A11})$$

To determine the form of the time-evolution operators $U_C(\alpha_j)$ of instantaneous global control pulses ($j = 1, 2, 3$), we utilize the well-known identity in Eq. (13). In this way, we obtain the expression

$$U_C(\alpha_j) = \prod_{n=1}^4 [\cos \alpha_j \mathbb{1}_{16} - i \sin \alpha_j \mathcal{A}_n^{(j)}], \quad (\text{A12})$$

where the operators $\mathcal{A}_n^{(j)}$ are defined in Eq. (A4). By making use of the binomial theorem, from the last equation we further obtain

$$U_C(\alpha_j) = \sum_{m=0}^4 (\cos \alpha_j)^{4-m} (-i \sin \alpha_j)^m \mathcal{S}_m^{(j)}, \quad (\text{A13})$$

where $\mathcal{S}_0^{(j)} = \mathbb{1}_{16}$ and the operators $\mathcal{S}_m^{(j)}$ ($m = 1, \dots, 4$) are constructed using the operators $\mathcal{A}_n^{(j)}$ according to

$$\mathcal{S}_m^{(j)} = \sum_{1 \leq n_1 < \dots < n_m \leq 4} \prod_{i=1}^m \mathcal{A}_{n_i}^{(j)}. \quad (\text{A14})$$

It is worthwhile to note that the last equation generalizes Eq. (A8), its three-qubit counterpart.

The next step in the derivation of the time-evolution operators $U_C(\alpha_j)$ corresponding to the instantaneous control pulses is to project the operators $S_m^{(j)}$ onto the symmetry-adapted basis of Eq. (A12); we denote by P_S the corresponding projector onto the five-dimensional permutationally invariant subspace of the four-qubit Hilbert space. In this manner, we obtain the following 5×5 matrices:

$$\begin{aligned}
P_S S_0^{(j)} P_S^\dagger &= \mathbb{1}_5, \\
P_S S_1^{(j)} P_S^\dagger &= \begin{pmatrix} 0 & 2e^{-i\phi_j} & 0 & 0 & 0 \\ 2e^{i\phi_j} & 0 & \sqrt{6} e^{-i\phi_j} & 0 & 0 \\ 0 & \sqrt{6} e^{i\phi_j} & 0 & \sqrt{6} e^{-i\phi_j} & 0 \\ 0 & 0 & \sqrt{6} e^{i\phi_j} & 0 & 2e^{-i\phi_j} \\ 0 & 0 & 0 & 2e^{i\phi_j} & 0 \end{pmatrix}, \\
P_S S_2^{(j)} P_S^\dagger &= \begin{pmatrix} 0 & 0 & \sqrt{6} e^{-2i\phi_j} & 0 & 0 \\ 0 & 3 & 0 & 3e^{-2i\phi_j} & 0 \\ \sqrt{6} e^{2i\phi_j} & 0 & 4 & 0 & \sqrt{6} e^{-2i\phi_j} \\ 0 & 3e^{2i\phi_j} & 0 & 3 & 0 \\ 0 & 0 & \sqrt{6} e^{2i\phi_j} & 0 & 0 \end{pmatrix}, \\
P_S S_3^{(j)} P_S^\dagger &= \begin{pmatrix} 0 & 0 & 0 & 2e^{-3i\phi_j} & 0 \\ 0 & 0 & \sqrt{6} e^{-i\phi_j} & 0 & 2e^{-3i\phi_j} \\ 0 & \sqrt{6} e^{i\phi_j} & 0 & \sqrt{6} e^{-i\phi_j} & 0 \\ 2e^{3i\phi_j} & 0 & \sqrt{6} e^{i\phi_j} & 0 & 0 \\ 0 & 2e^{3i\phi_j} & 0 & 0 & 0 \end{pmatrix}, \\
P_S S_4^{(j)} P_S^\dagger &= \begin{pmatrix} 0 & 0 & 0 & 0 & e^{-4i\phi_j} \\ 0 & 0 & 0 & e^{-2i\phi_j} & 0 \\ 0 & 0 & 1 & 0 & 0 \\ 0 & e^{2i\phi_j} & 0 & 0 & 0 \\ e^{4i\phi_j} & 0 & 0 & 0 & 0 \end{pmatrix}. \tag{A15}
\end{aligned}$$

Finally, after inserting the obtained matrices into Eq. (A13) and carrying out straightforward manipulations we can obtain the matrices representing the time-evolution operators $U_C(\alpha_j)$ in the chosen symmetry-adapted basis.

-
- [1] S. Dogra, K. Dorai, and Arvind, *Phys. Rev. A* **91**, 022312 (2015).
- [2] D. Das, S. Dogra, K. Dorai, and Arvind, *Phys. Rev. A* **92**, 022307 (2015).
- [3] C. Li and Z. Song, *Phys. Rev. A* **91**, 062104 (2015).
- [4] Y.-H. Kang, Y.-H. Chen, Z.-C. Shi, J. Song, and Y. Xia, *Phys. Rev. A* **94**, 052311 (2016).
- [5] Y.-H. Kang, Y.-H. Chen, Q.-C. Wu, B.-H. Huang, J. Song, and Y. Xia, *Sci. Rep.* **6**, 36737 (2016).
- [6] V. M. Stojanović, *Phys. Rev. Lett.* **124**, 190504 (2020).
- [7] J. Peng, J. Zheng, J. Yu, P. Tang, G. A. Barrios, J. Zhong, E. Solano, F. Albarrán-Arriagada, and L. Lamata, *Phys. Rev. Lett.* **127**, 043604 (2021).
- [8] V. M. Stojanović, *Phys. Rev. A* **103**, 022410 (2021).
- [9] J. Zheng, J. Peng, P. Tang, F. Li, and N. Tan, *Phys. Rev. A* **105**, 062408 (2022).
- [10] G. Q. Zhang, W. Feng, W. Xiong, Q. P. Su, and C. P. Yang, *Phys. Rev. A* **107**, 012410 (2023).
- [11] G. Q. Zhang, W. Feng, W. Xiong, D. Xu, Q. P. Su, and C. P. Yang, *arXiv:2302.06204*.
- [12] C. Song, K. Xu, W. Liu, C.-P. Yang, S.-B. Zheng, H. Deng, Q. Xie, K. Huang, Q. Guo, L. Zhang *et al.*, *Phys. Rev. Lett.* **119**, 180511 (2017).
- [13] M. Erhard, M. Malik, M. Krenn, and A. Zeilinger, *Nat. Photon.* **12**, 759 (2018).
- [14] V. Macrì, F. Nori, and A. F. Kockum, *Phys. Rev. A* **98**, 062327 (2018).
- [15] I. Dhand, M. Engelkemeier, L. Sansoni, S. Barkhofen, C. Silberhorn, and M. B. Plenio, *Phys. Rev. Lett.* **120**, 130501 (2018).
- [16] R.-H. Zheng, Y.-H. Kang, Z.-C. Shi, and Y. Xia, *Ann. Phys. (Leipzig)* **531**, 1800447 (2019).
- [17] J. Nogueira, P. A. Oliveira, F. M. Souza, and L. Sanz, *Phys. Rev. A* **103**, 032438 (2021).
- [18] Y.-F. Qiao, J.-Q. Chen, X.-L. Dong, B.-L. Wang, X.-L. Hei, C.-P. Shen, Y. Zhou, and P.-B. Li, *Phys. Rev. A* **105**, 032415 (2022).
- [19] W. Feng, G. Q. Zhang, Q. P. Su, J. X. Zhang, and C. P. Yang, *Phys. Rev. Appl.* **18**, 064036 (2022).
- [20] E. Pachniak and S. A. Malinovskaya, *Sci. Rep.* **11**, 12980 (2021).
- [21] S. H. Hauck, G. Alber, and V. M. Stojanović, *Phys. Rev. A* **104**, 053110 (2021).
- [22] S. H. Hauck and V. M. Stojanović, *Phys. Rev. Appl.* **18**, 014016 (2022).
- [23] R.-H. Zheng, Y.-H. Kang, D. Ran, Z.-C. Shi, and Y. Xia, *Phys. Rev. A* **101**, 012345 (2020).

- [24] T. Haase, G. Alber, and V. M. Stojanović, *Phys. Rev. A* **103**, 032427 (2021).
- [25] T. Haase, G. Alber, and V. M. Stojanović, *Phys. Rev. Res.* **4**, 033087 (2022).
- [26] J. K. Nauth and V. M. Stojanović, *Phys. Rev. A* **106**, 032605 (2022).
- [27] V. M. Stojanović and J. K. Nauth, *Phys. Rev. A* **106**, 052613 (2022).
- [28] X. Q. Shao, F. Liu, X. W. Xue, W. L. Mu, and W. Li, [arXiv:2303.13039](https://arxiv.org/abs/2303.13039).
- [29] J. P. Dowling and G. J. Milburn, *Phil. Trans. R. Soc. A* **361**, 1655 (2003).
- [30] F. Haas, J. Volz, R. Gehr, J. Reichel, and J. Esteve, *Science* **344**, 180 (2014).
- [31] N. Friis *et al.*, *Phys. Rev. X* **8**, 021012 (2018).
- [32] W. Dür, G. Vidal, and J. I. Cirac, *Phys. Rev. A* **62**, 062314 (2000).
- [33] D. M. Greenberger, M. A. Horne, and A. Zeilinger, in *Bell's Theorem, Quantum Theory, and Conceptions of the Universe* (Kluwer Academic, Dordrecht, The Netherlands, 1989), pp. 73–76.
- [34] M. A. Nielsen and I. L. Chuang, *Quantum Computation and Quantum Information* (Cambridge University Press, Cambridge, England, 2000).
- [35] R. H. Dicke, *Phys. Rev.* **93**, 99 (1954).
- [36] A. Neven, J. Martin, and T. Bastin, *Phys. Rev. A* **98**, 062335 (2018).
- [37] D. A. Lidar and K. B. Whaley, in *Irreversible Quantum Dynamics* (Springer, Berlin, 2003), pp. 83–120.
- [38] R. Prevedel, G. Cronenberg, M. S. Tame, M. Paternostro, P. Walther, M. S. Kim, and A. Zeilinger, *Phys. Rev. Lett.* **103**, 020503 (2009).
- [39] G. Toth, *Phys. Rev. A* **85**, 022322 (2012).
- [40] S. K. Özdemir, J. Shimamura, and N. Imoto, *New J. Phys.* **9**, 43 (2007).
- [41] A. M. Childs, E. Farhi, J. Goldstone, and S. Gutmann, *Quantum Inf. Comput.* **2**, 181 (2002).
- [42] D. B. Hume, C. W. Chou, T. Rosenband, and D. J. Wineland, *Phys. Rev. A* **80**, 052302 (2009).
- [43] P. A. Ivanov, D. Porras, S. S. Ivanov, and F. Schmidt-Kaler, *J. Phys. B: At. Mol. Opt. Phys.* **46**, 104003 (2013).
- [44] L. Lamata, C. E. López, B. P. Lanyon, T. Bastin, J. C. Retamal, and E. Solano, *Phys. Rev. A* **87**, 032325 (2013).
- [45] J. K. Stockton, R. van Handel, and H. Mabuchi, *Phys. Rev. A* **70**, 022106 (2004).
- [46] Y.-F. Xiao, X.-B. Zou, and G.-C. Guo, *Phys. Rev. A* **75**, 012310 (2007).
- [47] X.-Q. Shao, L. Chen, S. Zhang, Y.-F. Zhao, and K.-H. Yeon, *Europhys. Lett.* **90**, 50003 (2010).
- [48] W. Wieczorek, R. Krischek, N. Kiesel, P. Michelberger, G. Toth, and H. Weinfurter, *Phys. Rev. Lett.* **103**, 020504 (2009).
- [49] C. Wu, C. Guo, Y. Wang, G. Wang, X.-L. Feng, and J.-L. Chen, *Phys. Rev. A* **95**, 013845 (2017).
- [50] Y. Wang and B. M. Terhal, *Phys. Rev. A* **104**, 032407 (2021).
- [51] F. Solgun and S. Srinivasan, *Phys. Rev. Appl.* **18**, 044025 (2022).
- [52] For a review, see L. M. K. Vandersypen and I. L. Chuang, *Rev. Mod. Phys.* **76**, 1037 (2005).
- [53] L. Viola, E. Knill, and R. Laflamme, *J. Phys. A: Math. Gen.* **34**, 7067 (2001).
- [54] J. Zhang, D. Burgarth, R. Laflamme, and D. Suter, *Phys. Rev. A* **91**, 012330 (2015).
- [55] M. D. Shulman, O. E. Dial, S. P. Harvey, H. Bluhm, V. Umansky, and A. Yacoby, *Science* **336**, 202 (2012).
- [56] J. Levy, *Phys. Rev. Lett.* **89**, 147902 (2002).
- [57] For an extensive review, see, e.g., M. Morgado and S. Whitlock, *AVS Quantum Sci.* **3**, 023501 (2021).
- [58] For an up-to-date review, see X.-F. Shi, *Quantum Sci. Technol.* **7**, 023002 (2022).
- [59] X. X. Li, J. B. You, X. Q. Shao, and W. Li, *Phys. Rev. A* **105**, 032417 (2022).
- [60] F. Albertini and D. D'Alessandro, *J. Math. Phys.* **59**, 052102 (2018).
- [61] J. A. Jones, *Phys. Rev. A* **67**, 012317 (2003).
- [62] C. D. Hill, *Phys. Rev. Lett.* **98**, 180501 (2007).
- [63] M. R. Geller, E. J. Pritchett, A. Galiatdinov, and J. M. Martinis, *Phys. Rev. A* **81**, 012320 (2010).
- [64] J. Ghosh and M. R. Geller, *Phys. Rev. A* **81**, 052340 (2010).
- [65] See, e.g. T. Tanamoto, *Phys. Rev. A* **88**, 062334 (2013).
- [66] T. Tanamoto, D. Becker, V. M. Stojanović, and C. Bruder, *Phys. Rev. A* **86**, 032327 (2012).
- [67] T. Tanamoto, V. M. Stojanović, C. Bruder, and D. Becker, *Phys. Rev. A* **87**, 052305 (2013).
- [68] D. Stefanatos and E. Paspalakis, *Phys. Rev. A* **102**, 052618 (2020).
- [69] R. Raussendorf and H. J. Briegel, *Phys. Rev. Lett.* **86**, 5188 (2001).
- [70] D. D'Alessandro, *Introduction to Quantum Control and Dynamics* (Taylor & Francis, Boca Raton, FL, 2008).
- [71] X. Wang, D. Burgarth, and S. G. Schirmer, *Phys. Rev. A* **94**, 052319 (2016).
- [72] J. Zhang and K. B. Whaley, *Phys. Rev. A* **71**, 052317 (2005).
- [73] P. Zanardi, *Phys. Rev. A* **60**, R729(R) (1999).
- [74] P. Ribeiro and R. Mosseri, *Phys. Rev. Lett.* **106**, 180502 (2011).
- [75] A. Burchardt, J. Czartowski, and K. Zyczkowski, *Phys. Rev. A* **104**, 022426 (2021).
- [76] D. W. Lyons, J. R. Arnold, and A. F. Swogger, *Phys. Rev. A* **105**, 032442 (2022).
- [77] T. F. Gallagher, *Rydberg Atoms* (Cambridge University Press, Cambridge, England, 1994).
- [78] T. M. Graham, M. Kwon, B. Grinkemeyer, Z. Marra, X. Jiang, M. T. Lichtman, Y. Sun, M. Ebert, and M. Saffman, *Phys. Rev. Lett.* **123**, 230501 (2019).
- [79] For the reference material, see the following: <https://docs.scipy.org/doc/scipy/reference/generated/scipy.optimize.minimize.html>.
- [80] For a recent review on optical tweezer arrays, see A. M. Kaufman and K.-K. Ni, *Nat. Phys.* **17**, 1324 (2021).
- [81] J. K. Stockton, J. M. Geremia, A. C. Doherty, and H. Mabuchi, *Phys. Rev. A* **67**, 022112 (2003).
- [82] V. M. Stojanović, A. Fedorov, A. Wallraff, and C. Bruder, *Phys. Rev. B* **85**, 054504 (2012).

- [83] V. M. Stojanović, M. Vanević, E. Demler, and L. Tian, *Phys. Rev. B* **89**, 144508 (2014).
- [84] V. M. Stojanović and I. Salom, *Phys. Rev. B* **99**, 134308 (2019).
- [85] J. K. Nauth and V. M. Stojanović, *Phys. Rev. B* **107**, 174306 (2023).
- [86] R. Heule, C. Bruder, D. Burgarth, and V. M. Stojanović, *Phys. Rev. A* **82**, 052333 (2010).
- [87] R. Heule, C. Bruder, D. Burgarth, and V. M. Stojanović, *Eur. Phys. J. D* **63**, 41 (2011).
- [88] See, e.g., V. M. Stojanović, *Phys. Rev. A* **99**, 012345 (2019).